Prion protein lowering is a disease-modifying therapy across prion strains, disease stages, and endpoints

Eric Vallabh Minikel[1,2,3,4,5], Hien T Zhao[6], Jason Le[7], Jill O'Moore[8], Rose Pitstick[8], Samantha Graffam[7], George A Carlson[8], Jasna Kriz[9], Jae Beom Kim[10], Jiyan Ma[11], Holger Wille[12], Judd Aiken[12], Deborah McKenzie[12], Katsumi Doh-ura[13], Matthew Beck[7], Rhonda O'Keefe[7], Jacquelyn Stathopoulos[7], Tyler Caron[7], Stuart L Schreiber[7,14], Jeffrey B Carroll[15], Holly B Kordasiewicz[6,†], Deborah E Cabin[8,†], Sonia M Vallabh[1,2,3,4,5,†]

1. Stanley Center for Psychiatric Research, Broad Institute of MIT and Harvard, Cambridge, MA, 02142, USA
2. Prion Alliance, Cambridge, MA, 02139, USA
3. Henry and Allison McCance Center for Brain Health, Massachusetts General Hospital, Boston, MA, 02114, USA
4. Department of Neurology, Massachusetts General Hospital, Boston, MA, 02114, USA
5. Harvard Medical School, Boston, MA, 02115, USA
6. Ionis Pharmaceuticals Inc, Carlsbad, CA, 92010, USA
7. Broad Institute of MIT and Harvard, Cambridge, MA, 02142, USA
8. McLaughlin Research Institute, Great Falls, MT, 59405, USA
9. Cervo Brain Research Center, Université Laval, Québec, QC, G1J 2G3, Canada
10. PerkinElmer, Hopkinton, MA, 01748, USA
11. Center for Neurodegenerative Science, Van Andel Institute, Grand Rapids, MI, 49503, USA
12. University of Alberta, Edmonton, AB, T6G 2M8, Canada
13. Department of Neurochemistry, Tohoku University Graduate School of Medicine, Sendai, Miyagi, 980-8575, Japan
14. Department of Chemistry & Chemical Biology, Harvard University, Cambridge, MA, 02138, USA
15. Western Washington University, Bellingham, WA, 98225, USA

†To whom correspondence should be addressed: svallabh@broadinstitute.org, deborahcabin@mclaughlinresearch.org, or hkordasiewicz@ionisph.com

Abstract

Lowering of prion protein (PrP) expression in the brain is a genetically validated therapeutic hypothesis in prion disease. We recently showed that antisense oligonucleotide (ASO)-mediated PrP suppression extends survival and delays disease onset in intracerebrally prion-infected mice in both prophylactic and delayed dosing paradigms. Here, we examine the efficacy of this therapeutic approach across diverse paradigms, varying the dose and dosing regimen, prion strain, treatment timepoint, and examining symptomatic, survival, and biomarker readouts. We recapitulate our previous findings with additional PrP-targeting ASOs, and demonstrate therapeutic benefit against four additional prion strains, with no evidence for the development of drug resistance. We demonstrate that less than 25% PrP suppression is sufficient to extend survival and delay symptoms in a prophylactic paradigm. Both neuroinflammation measured through live animal bioluminescence imaging and neuronal injury measured by plasma neurofilament light chain can be reversed by a single dose of PrP-lowering ASO administered after the detection of pathological change in these biomarkers. Chronic ASO-mediated suppression of PrP beginning at any time up to early signs of neuropathology confers benefit similar to constitutive heterozygous PrP knockout. Remarkably, even after emergence of frank symptoms including weight loss, a single treatment prolongs survival by months in a subset of animals. Taken together, these results support ASO-mediated PrP lowering, and PrP-lowering therapeutics in general, as a promising path forward against prion disease.

Introduction

Prion disease, a rapidly fatal and currently untreatable neurodegenerative disease, is caused by the post-translational conformational corruption of host-encoded prion protein (PrP)[1]. Due to its central role in disease pathophysiology, reduction of native PrP is an attractive therapeutic hypothesis in prion disease[2]. Homozygous deletion of PrP prevents prion infection[3,4], while heterozygous PrP knockout delays development of disease following prion infection[4–7] and transgenic PrP overexpression accelerates it[8], providing genetic evidence of a continuous dose-response relationship between PrP dosage and disease susceptibility. Conditional knockout systems have confirmed that post-natal depletion confers significant survival benefit, even in the presence of low levels of residual PrP expression[9,10]. Knockout animals are healthy[11–13]. The only established knockout phenotype is a peripheral neuropathy, apparently due to deficiency of myelin maintenance signaling to a Schwann cell receptor[14], which is histologically evident yet phenotypically mild to undetectable in homozygotes and is not observed in heterozygotes[15,16]. Heterozygous inactivating mutations also appear to be tolerated in humans[17,18], minimizing any concern about on-target toxicity of pharmacologic PrP lowering.

The use of therapeutic oligonucleotides to lower PrP by targeting its RNA has been considered for over two decades[19], but early attempts, hampered by drug delivery and distribution challenges, yielded modest or no benefit in animal models[20–24]. Genetically targeted therapies designed to reduce levels of other single target proteins have recently shown promising target engagement in the human central nervous system[25–27]. Building on these successes, we and others recently showed that PrP-lowering antisense oligonucleotides (ASOs), bolus dosed into cerebrospinal fluid (CSF), can extend survival by 61-98% in prion-infected mice[28].

For PrP-lowering therapy to advance effectively, a number of fundamental questions must be addressed. While heterozygous knockout animals show a clear benefit to 50% PrP reduction[4–7], the minimal threshold of PrP knockdown needed to confer benefit has not been established. The existence of different prions strains, or subtypes, has complicated previous drug development efforts: antiprion compounds with non-PrP-lowering mechanisms of action have failed to generalize across strains[29–33], and prions have been shown capable of adapting to drug treatment, giving rise to new drug-resistant strains[30,34,35]. It is therefore critical to test any potential prion disease therapeutic strategy against multiple prion strains, and to monitor for development of drug-resistant prions. While our previous experiments showed the delay of pathological changes to brain tissue of ASO-treated animals[28], we did not investigate potential impact on established neuropathological changes following treatment. Further, our prior experiments relied on a limited number of ASO doses, rather than chronic dosing aiming for continuous suppression, though the latter paradigm better mirrors clinical use of ASOs. Finally, in prion disease it is important to understand at what disease stage treatment can be effective. Clinically, most prion disease patients die within half a year of first symptoms[36], and this rapid decline is mirrored by high levels of biofluid neuronal injury and prion seeding biomarkers in the symptomatic phase of disease[37–42]. Meanwhile, individuals at risk for genetic prion disease, caused by protein-altering variants in the prion protein gene (*PRNP*), can be identified through predictive genetic testing when disease onset is on expectation years or decades away[43], ahead of molecular markers of pathology[44]. This spectrum motivates investigation of a range of treatment timepoints relative to prion inoculation, development of molecular pathology, and presentation of frank symptoms to explore the potential of PrP-lowering treatment.

Here, using ASOs as tool compounds, we test the efficacy of PrP lowering across a variety of therapeutic paradigms in prion-infected mice, in order to fill these critical knowledge gaps and inform the clinical development of PrP-lowering drugs.

Results

Therapeutic benefit and mechanism of action replicate across ASO chemistries.

ASOs can be synthesized with diverse combinations of sugar, backbone, and other chemical modifications[45]. Survival benefits in prion-infected mice have been previously demonstrated for three PrP-targeting sequences with two chemical formulations[22,28]. Motivated by the desire to additionally test the ASO chemistry now in clinical trials for Huntington's disease and Amyotrophic lateral sclerosis (ALS) with SOD1 mutations[25,46], we designed and synthesized two new PrP-targeting and one new control ASO (Table S1) and sought to replicate previous findings. These compounds (ASOs 4 – 6) achieved similar levels of target engagement as those previously reported, with active sequences reducing cortical PrP RNA by approximately half within one week after a 500 µg dose (Figure S1).

We studied the efficacy of ASOs in intracerebrally prion-inoculated mice in experiments variously utilizing either a symptomatic endpoint (euthanasia upon observation of five pre-specified neurological symptoms; see Methods) or a more advanced terminal disease endpoint (euthanasia upon 15-20% body weight loss or inability to reach food and water; see Methods). These paradigms respectively allow for early halting of experiments when animals have become moderately ill, or for the potential to observe changes in the rate of symptomatic progression towards end-stage disease.

In a prophylactic experiment as previously described[28], intracerebroventricular (ICV) ASO treatments were administered at 14 days prior to and again at 76 days post-infection (dpi) with Rocky Mountain Lab (RML) prions[47], a widely used laboratory prion strain[48]. Groups of N=10 C57BL/6N mice received two 500 µg doses of active ASO 5, active ASO 6, control ASO 4, or saline by stereotactic ICV injection. Active ASOs 5 and 6 closely replicated the survival benefit reported with active ASOs 1 and 2[28], delaying symptomatic endpoint by 108% and 80% respectively compared to saline (median 314 and 270 vs. 150 dpi) (Figure 1A). These PrP-lowering ASOs delayed onset of disease as reflected in weight loss (Figure 1B) and symptom accumulation (Figure 1C) in treated animals. In a delayed treatment experiment mirroring that reported previously[28], a single 500 µg bolus dose was administered at 120 dpi, or ~72% of the time to terminal disease endpoint. This terminal endpoint was delayed by 68% for active ASO 6 (median 277 vs. 165 dpi; Figure 1D), with all mice surviving beyond the point when all of the saline-treated animals had died, while weight loss was partially reversed and symptom accumulation attenuated (Figure 1E-F). Active ASO 5 was not tolerated at this timepoint (Figure 1D), replicating the ASO-specific, disease stage-dependent toxicity reported previously[22,28]. Across both prophylactic and delayed treatment paradigms, non-targeting control ASO 4 conferred no survival benefit (Figure 1A, 1D), replicating control ASO 3 results[28] and confirming PrP lowering as the mechanism of action by which ASOs antagonize prion disease[28,49]. In both of these experiments, with blinded assessments (see Methods), we recapitulated our previous findings, demonstrating that ASO-mediated PrP lowering extended survival and delayed disease course, in both prophylactic and delayed treatment paradigms. Given the comparable results across tool compounds of different chemistries, active ASOs 1 and 6 were used interchangeably in the experiments that follow.

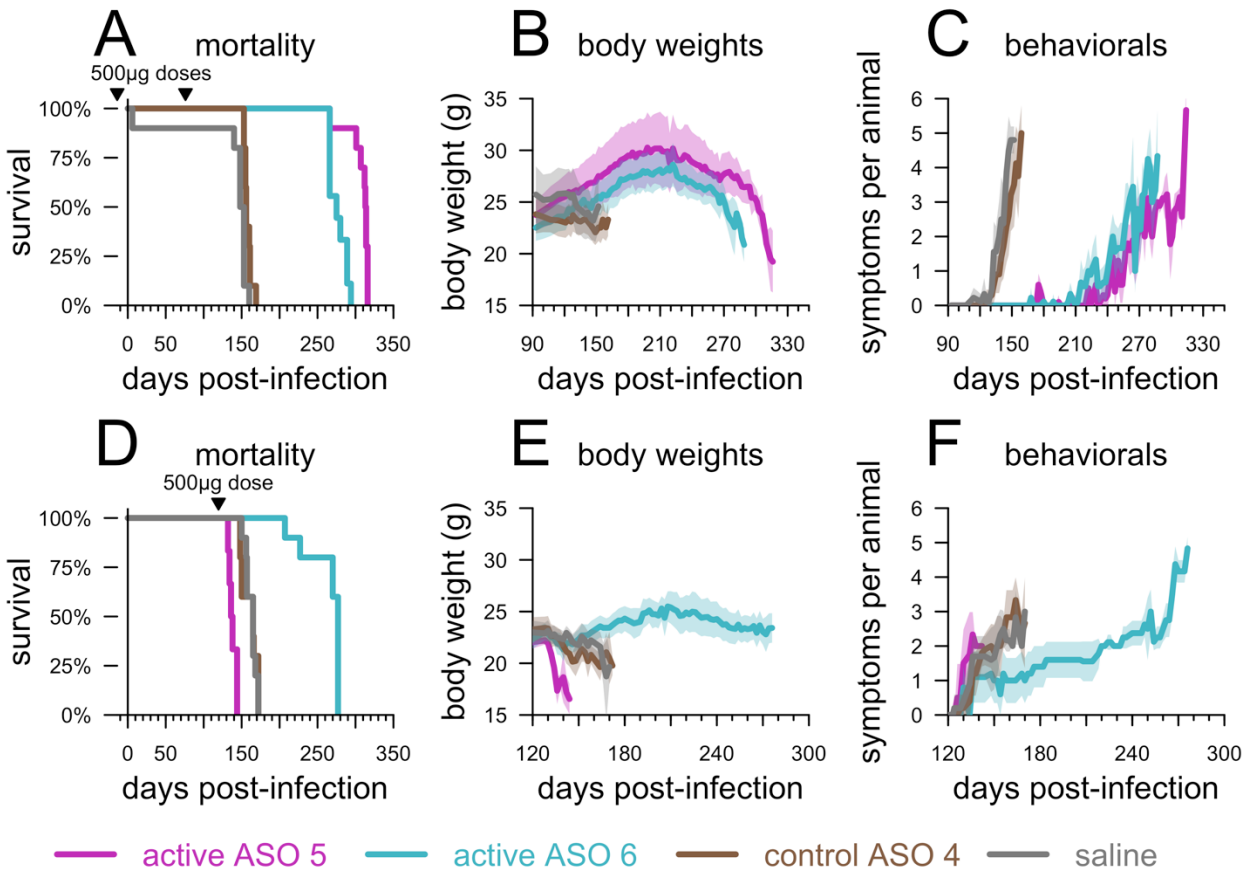

Figure 1. Replication of early and late treatment efficacy of ASOs. *Survival* ***(A,D)****, body weights* ***(B,E)****, and symptom trajectories* ***(C,F)*** *of mice treated with ASOs prophylactically (-14 and 76 dpi)* ***(A-C)*** *or at 120 dpi* ***(D-F)****.*

Dose-responsive benefits to PrP-lowering

We next investigated the minimum level of PrP suppression sufficient to confer benefit in prion-inoculated mice. We characterized the extent of PrP lowering by injecting ASO1 into wild-type, uninfected mice at 6 doses (0-700 µg). PrP mRNA in the cortex at 2 weeks post-dose was dose-dependently lowered, with residual PrP ranging from 79% at the 30 µg dose to 39% at the 700 µg dose compared to vehicle-treated animals (Figure 2A). As target engagement at the 500 and 700 µg doses was not significantly different, the 0 through 500 µg doses were selected for a survival study in RML prion-infected mice per prophylactic paradigm described above (two doses, at -14 and 76 dpi) utilizing a symptomatic endpoint assessed by blinded raters. Across doses of 0 (saline), 30, 100, 300, or 500 µg of active ASO 1, PrP reduction tracked with incubation time in animals that ultimately succumbed to prion disease (Figure 2B), with a significant increase in time to symptomatic endpoint even at 21% knockdown (median 173 vs. 152 dpi at 30 µg, $P = 0.002$, two-sided log-rank test). Across all doses, overall survival was increased in step with PrP knockdown (Figure 2C) and attendant delays in weight loss (Figure 2D), accumulation of prion disease symptoms (Figure 2E), and decline in nest-building (Figure 2F) suggested that at all doses tested, the treatment had extended healthy life. Thus, dose-dependent PrP lowering translated to dose-dependent benefit in prion disease, with as little as 21% PrP knockdown extending survival.

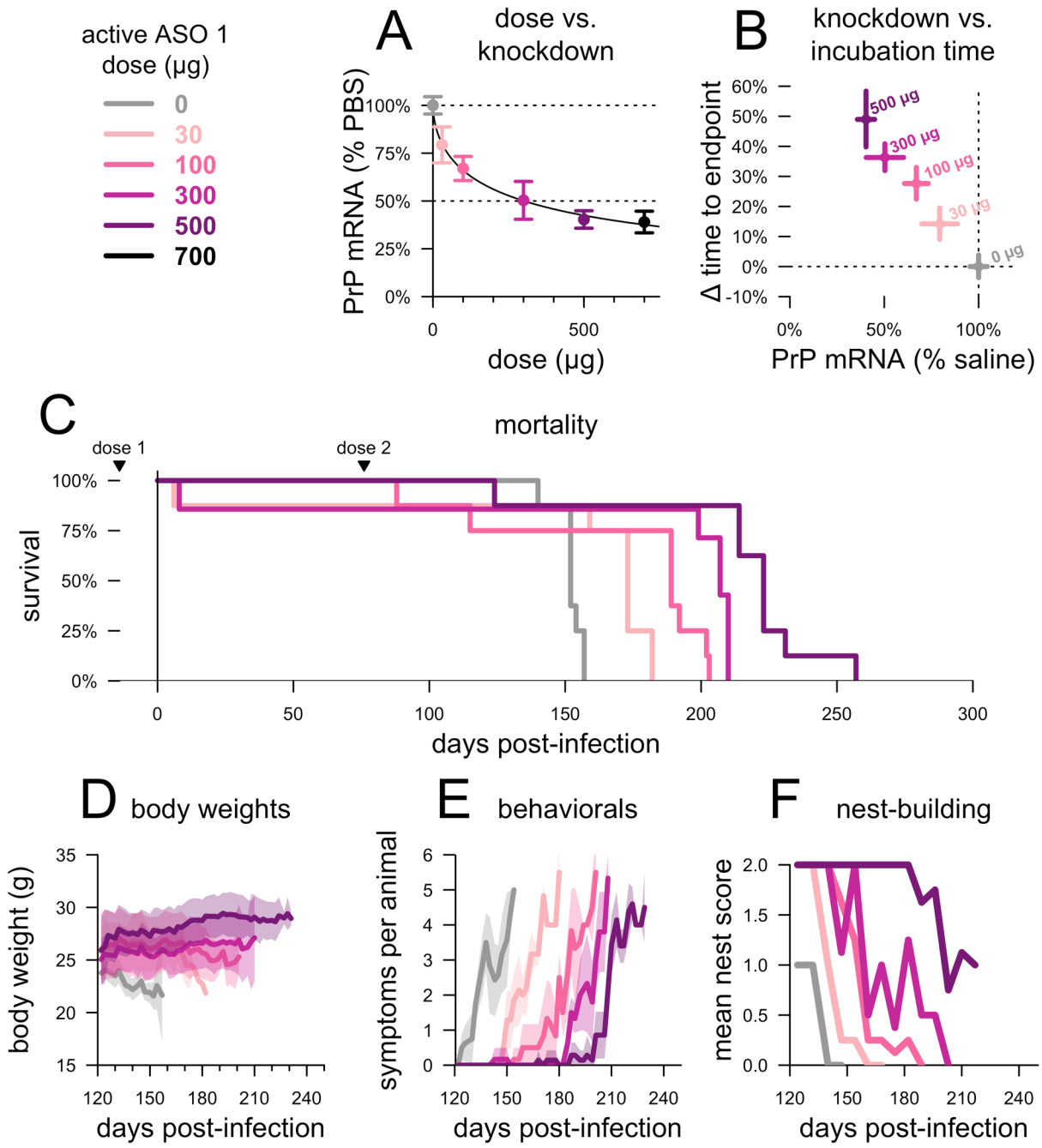

Figure 2. Relationship between degree of PrP lowering and therapeutic benefit. A) *Dose versus ipsilateral cortical PrP mRNA knockdown determined by qPCR at 2 weeks post-treatment and normalized to the mean of saline-treated, non-infected animals, N=3 per group,* ***B)*** *PrP mRNA knockdown (from panel A) versus time to symptomatic endpoint in groups of N=8 prion-infected animals receiving two injections of the indicated dose, at -14 and 76 dpi, and, for the same animals,* ***C)*** *overall mortality,* ***D)*** *body weights normalized to each mouse's individual weight at 122 dpi,* ***E)*** *mean symptom count per animal, and* ***F)*** *mean nest score. Studies conducted at the Broad Institute.*

Efficacy of PrP lowering across prion strains

As all prion strains share the common substrate of PrP, we hypothesized that reduction of PrP, by either genetic or pharmacologic means, would effectively modify prion disease across strains. To test this hypothesis, we challenged mice with five different previously characterized mouse-adapted laboratory prion strains of diverse origins: RML (adapted from goat scrapie)[47], 22L (sheep scrapie)[50], ME7 (sheep scrapie)[51], Fukuoka-1 (human P102L GSS)[52], and OSU (synthetic)[53].

In the pharmacological treatment arm, groups of mice infected with these prion strains received 500 µg ASO 1 at -14 and 76 dpi or saline (N=8 per treatment per strain). In the genetic control arm, heterozygous ZH3 PrP knockout[54] (*Prnp*$^{+/-}$) or wild-type mice (N=8 per genotype per strain) were inoculated with the same five prion strains listed above without pharmacologic intervention. Mice in both arms were followed to a symptomatic endpoint by blinded raters. Across strains, disease was delayed and survival extended in animals with reduced PrP, whether the reduction was ASO-mediated (Table 1, Figure S2) or genetic (Table 1, Figure S3). Survival time response to ASO treatment across strains ranged from +24% to +46%, while the increase in survival time due to heterozygous PrP knockout ranged from +63% to +163% (Table 1), with differences among strains reflected in overall mortality and in trajectories of body weight loss, symptom accumulation and nest-building (Figure S3). Overall, prophylactic PrP lowering by genetic or pharmacologic means proved effective against all five strains tested.

To test whether ASO treatment gives rise to drug-resistant prion strains, we prepared brain homogenate from terminally sick, RML prion-infected, active ASO 1-treated animals included in a previous experiment[28] (see Methods). Groups of N=8 mice inoculated with this prion isolate, termed RML[ASO] following established nomenclature[30], received two doses of 500 µg active ASO 1 or saline per the described prophylactic paradigm. Active ASO 1 retained its efficacy in this paradigm, delaying symptomatic endpoint by 74% (Table 1, Figure S2), similar to the 61% delay in the experiment from which the RML[ASO] isolate was sourced[28], suggesting that ASO treatment does not give rise to drug-resistant prion strains.

We next sought to compare the effect of PrP-lowering treatment across multiple strains in delayed treatment. We chose intervention timepoints for each strain estimated to be after ~80% of the incubation time had elapsed, based upon the previous experiment (Table 1), thus roughly corresponding to the 120 dpi timepoint where we and others observed efficacy against RML prions (Figure 1 and ref. [28]). At the chosen timepoint (122-129 dpi), each group of N=8 mice received one dose of 500 µg of active ASO 6 or saline and was followed to a symptomatic endpoint, again by blinded raters (see Methods). At this timepoint, active ASO 6 remained effective against all five prion strains (Table 2). In terms of increase in mean survival time, the ASO appeared highly effective against some strains and marginally effective against others (Table 2), however, inspection of survival curves (Figure S4A) revealed that differences were driven not by differences in maximum survival time, but by the proportion of ASO-treated animals that outlived their saline-treated counterparts. Accordingly, for each strain, we applied a cutoff of survival 10% beyond the mean of saline-treated controls (Table 2, right panel), corresponding to 1.96 standard deviations of control survival, when 95% of control animals would be expected to have reached endpoint. The differences in the proportions of ASO-treated animals crossing this threshold were not significantly different between strains (P = 0.80, two-sided Fisher exact test) and, among these animals, the overall survival time increase was similar across strains (+46% to +57%). Across strains, for treated animals that outlived controls, body weights declined initially and then partly rebounded (Figure S4B), first symptoms emerged

on a timeline similar to controls but further symptoms accumulated more slowly (Figure S4C), and nest building was somewhat impaired in the treated animals, with some variability between strains (Figure S4D). Overall, efficacy of late PrP-lowering treatment was confirmed across all five strains tested.

	ASO treatment experiment					genetic experiment				
	saline		active ASO 1		Δ	wild-type		*Prnp*$^{+/-}$		Δ
strain	days	*N*	days	*N*		days	*N*	days	*N*	
RML	153±4	7	211±3	8	+38%	150±5	4	396±83	7	+163%
22L	171±6	8	250±11	8	+46%*	161±6	7	270±11	8	+67%
Fukuoka-1	159±4	7	217±7	7	+37%	153±16	7	250±31	7	+63%
ME7	160±14	6	199±10	6	+24%	146±11	7	288±19	7	+98%
OSU	152±6	8	206±9	7	+36%	151±4	7	344±60	7	+128%
RML[ASO]	159±4	7	277±17	6	+74%					

Table 1. PrP lowering is effective across prion strains. *Days (mean±sd) to symptomatic endpoint for animals that received two 500 µg doses of ASO vs. saline, at -14 and at 76 dpi (left, details in Figure S2), or for untreated Pmp*$^{+/-}$ *vs. wild-type animals (right, details in Figure S3). Following established nomenclature*[30]*, RML[ASO] denotes prions from the brains of mice infected with RML prions and treated with ASOs (see Methods). Studies conducted at the Broad Institute. *Results from repeat experiment, see Figure S2 for details.*

	intervention timepoint		saline		active ASO 6		overall	active ASO 6 animals surviving >10% longer than saline mean		
strain	dpi	relative	days	N	days	N	Δ	proportion	days	Δ
RML	123	75%	164±7	6	189±54	8	+15%	3/8	251±17	+53%
22L	127	78%	164±5	8	235±43	7	+44%	6/7	251±5	+54%
Fukuoka-1	128	77%	166±14	8	255±4	3*	+54%	3/3	255±4	+54%
ME7	129	81%	160±11	8	179±52	8	+12%	3/8	234±45	+46%
OSU	122	77%	159±6	8	204±60	7	+28%	4/7	250±17	+57%

Table 2. PrP lowering is effective in delayed intervention against multiple prion strains. *Mice were infected with any of five prion strains and then treated with 500 µg ASO, or saline, at a pre-specified timepoint expected to be 80% of the way through the control group incubation period based on a previous experiment (Table 1). Actual treatment timepoints ranged from 75% - 81% of the incubation period. Overall Δ indicates difference in time to terminal endpoint counting all animals. The rightmost three columns show statistics on those ASO-treated animals that survived at least 10% longer than the mean of the saline animals for each strain. Details visualized in Figure S4. Studies conducted at the Broad Institute. *One of two cages intended for the Fukuoka-1 active cohort was lost to experimental error, resulting in a lower N for this group.*

Natural history of RML prion infection

In order to establish the pathological context of different treatment timepoints, we endeavored to systematically map biomarker, weight, and behavioral changes onto the incubation period by comparing N=12 RML prion-infected mice and N=12 uninoculated controls. Rotarod performance, an early sign in some prion models[55], and neurofilament light (NfL) in blood, an early sentinel biomarker of more slowly progressive neurodegenerative diseases in both mice[56] and humans[57,58], were evaluated at -7 dpi and every 30 days following inoculation. Weights, nest-building activity and a battery of symptomatic and behavioral observations (Table S2) were evaluated as the animals approached terminal endpoint.

Overall, group-wise symptomatic changes became apparent at approximately 120 dpi (Figure 3). Across 40 symptomatic and behavioral observations conducted (Table S2), the mean number of observations with score >0 became nominally elevated in RML mice at 116 dpi and unambiguously elevated by 135 dpi (P = 0.017 and P = 0.0010 respectively, two-sided Kolmogorov-Smirnov tests, Figure 3A). No individual observation measure showed any earlier sensitivity, with clear changes only at 135 dpi in abnormal activity level (slow), no balance on bar, and tail suspension: poor or no splay (Figure S5). Nest-building was impaired in all prion-infected cages by 120 dpi, though with just N=3 cages per group the significance of this remained ambiguous (P = 0.10, two-sided Kolmogorov-Smirnov test, Figure 3B). Weight loss, relative to each animal's baseline weight, achieved nominal significance in some but not all weighing sessions from 94 dpi onward, but became unambiguous only at 148 dpi (Figure 3C). Rotarod performance in prion-infected mice, normalized to each mouse's own baseline, began to show nominal decline at 120 dpi (P = 0.028, Figure 3D) strengthening by 150 dpi (P = 0.0024, Figure 3D). Even as these differences became apparent on a group-wise basis, distributions of both weights and rotarod latencies overlapped until some animals began to reach endpoint (Figure S6A-B). In contrast to these symptomatic measures, molecular evidence of pathology was detectable far sooner. Plasma NfL was nominally increased in prion-infected mice at 60 dpi (P = 0.015, two-sided Kolmogorov-Smirnov test), with a subset of mice elevated while the distributions still overlapped (Figure S6C). By 90 dpi, plasma NfL levels showed clear elevation in prion-infected mice, with non-overlapping distributions (Figure 3E and S6C) preceding frank symptoms. All changes grew in magnitude until the prion-infected mice reached endpoint at a median of 163 dpi (Figure 3F).

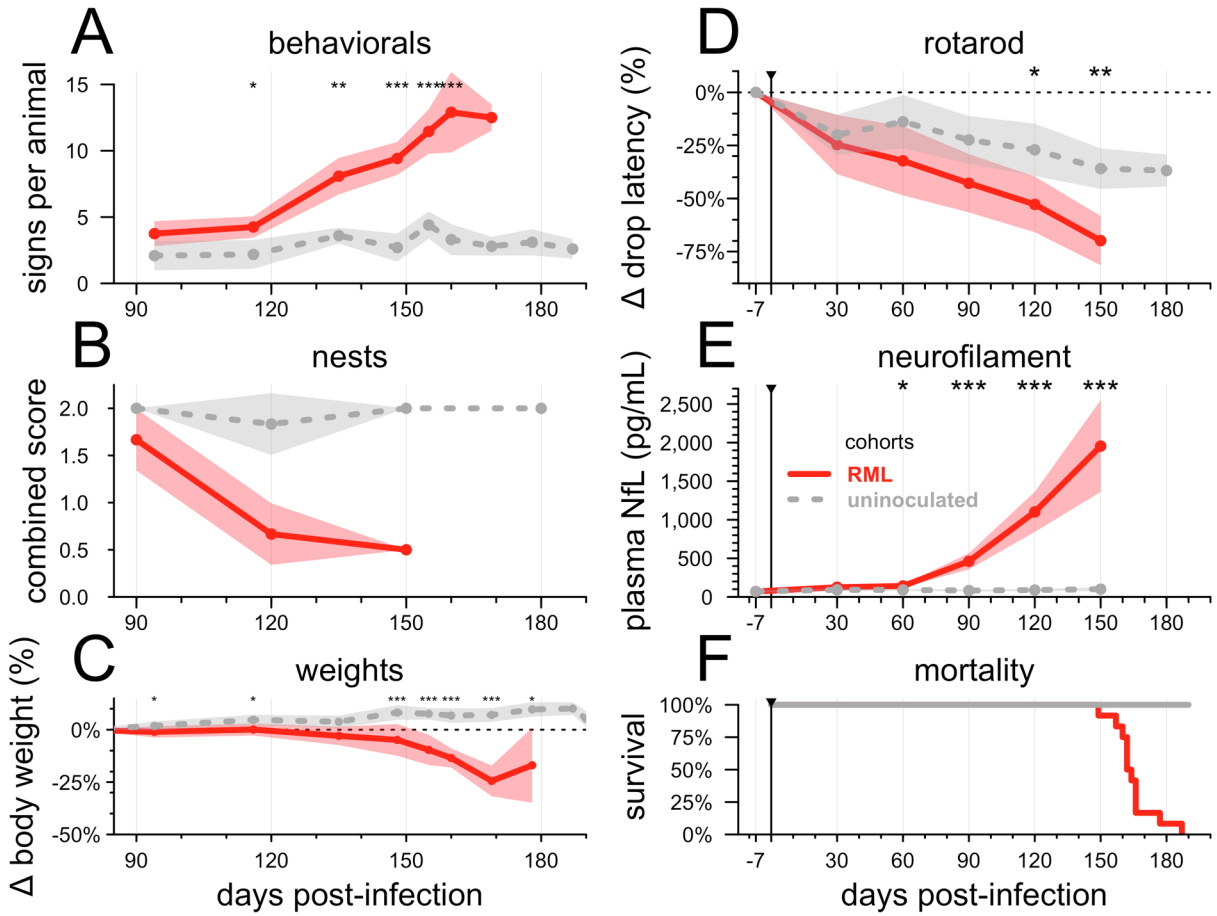

Figure 3. Natural history of RML prion infection. *N=12 mice infected with 30 µL of a 1% RML brain homogenate versus N=12 uninoculated controls. In panels A-E, lines represent means, shaded areas represent 95% confidence intervals of the mean, and dots represent assessment timepoints. Nominal statistical significance thresholds are displayed as: * P < 0.05, ** P < 0.01, *** P < 0.001.* ***A)*** *symptom accumulation (see Figure S5 and Table S2 for details),* ***B)*** *nest-building scores,* ***C)*** *weight change relative to each animal's 78 dpi baseline (see raw individual weights in Figure S6A)†,* ***D)*** *rotarod performance relative to each animal's -7 dpi baseline (see raw individual latencies in Figure S6B),* ***E)****, plasma NfL (see raw individual NfL trajectories in Figure S6C), and* ***F)*** *overall mortality. †In panel C, prion-infected animals that reached endpoint between planned assessments and were weighed a final time prior to euthanasia are grouped together with animals at the next planned assessment timepoint — for example, animals that reached endpoint at 166 dpi are averaged into the 169 dpi timepoint. Studies conducted at McLaughlin Research Institute.*

Biomarker response in mice treated at a pathological timepoint

Having characterized the time course of pathology, we evaluated whether and how biomarkers of pathology respond to PrP-lowering treatment. To evaluate NfL response to treatment, groups of N = 10 mice were inoculated with RML prions, and received a single ICV bolus dose of ASO 6 or saline at 120 dpi. Plasma NfL was quantified from bleeds taken at -1 dpi, 90 dpi, 119 dpi (one day pre-dose), 127 dpi (one week post-dose), and then every 30 days from 150 dpi onward. As expected, plasma NfL levels steadily rose through terminal illness in saline-treated animals (Figure 4A). In contrast, by 30 days after ASO treatment, plasma NfL levels fell significantly in

ASO-treated mice compared to the immediate pre-dose timepoint, suggesting a reversal of pathology driving the 53% increase in survival time (median 248 vs. 162 days, Figure 4B). NfL began to rebound ~90 days post-treatment, coincident with expected waning of the pharmacodynamic effect of ASOs[28] (Figure 4A). This experiment provided biomarker evidence that ASO-mediated PrP lowering can reverse pathology after disease-associated changes have begun to occur. To our knowledge, this is the first time pharmacological reversal of a translatable biomarker of disease has been demonstrated in a prion-infected animal.

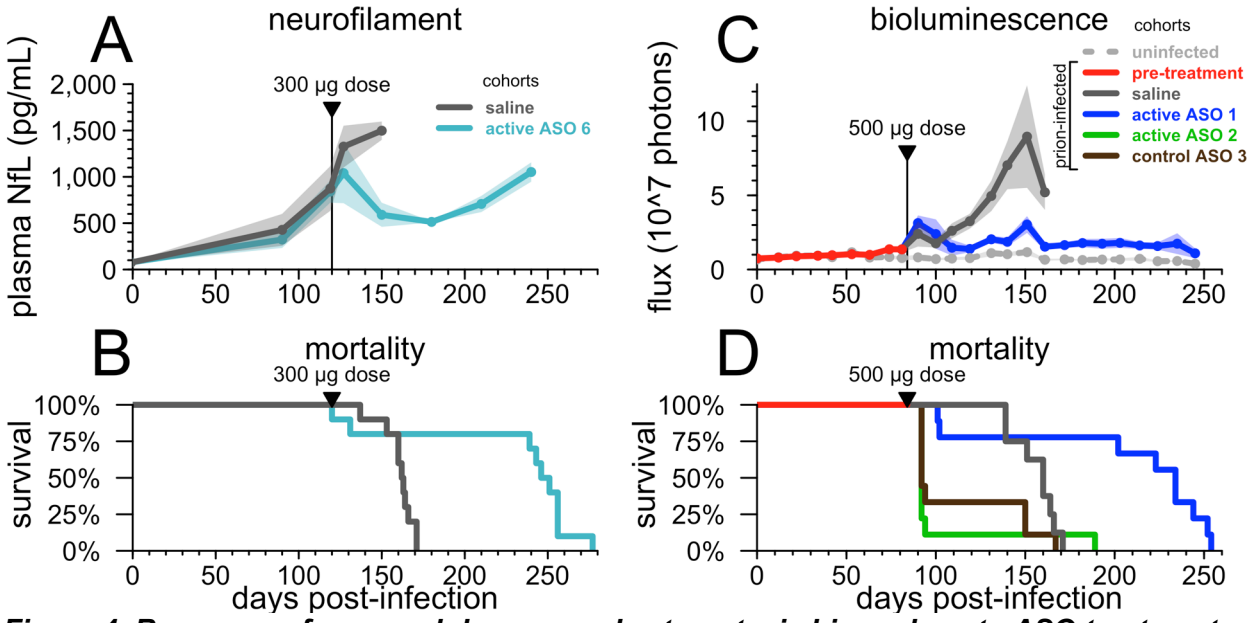

Figure 4. Response of neuronal damage and astrocytosis biomarkers to ASO treatment at a pathological timepoint. A) *plasma NfL and* ***B)*** *survival in wild-type mice infected with prions and dosed at 120 dpi, a timepoint at which the natural history study (Figure 3D) had indicated that NfL was dramatically elevated and rotarod performance and nest-building might be impaired. N=10 per group, of which NfL was assessed in N=10 saline-treated and N=5 active ASO 6-treated animals.* ***C)*** *live animal bioluminescence and* ***D)*** *survival in Tg(Gfap-luc) mice infected with prions and dosed at 83-84 dpi, after two consecutive imaging sessions showed elevated luminescence in the RML group compared to uninfected controls. N=9 per treatment group plus N=14 uninfected controls. Studies conducted at McLaughlin Research Institute.*

Reactive gliosis associated with increased expression of the astroglial intermediate filament gene *Gfap* has been previously established as one of the earliest neuropathological changes in prion-infected mice[59]. Using Tg(*Gfap*-luc) mice[60], which express luciferase under the *Gfap* promoter, it is possible to track the progression of gliosis by live animal bioluminescence imaging (BLI) throughout the course of prion disease[61] and to obtain time-series data on the effect of drug treatment[31]. To evaluate astroglial proliferation, we imaged N=36 Tg(*Gfap*-luc) RML prion-infected and N=14 uninfected mice by BLI every 7-11 days, and pre-specified that a single 500 µg dose of ASO 1, 2 or 3 would be administered after two consecutive imaging sessions showed a nominally significant ($P < 0.05$ by a two-sided Kolmogorov-Smirnov test) difference in BLI between infected and uninfected mice. Significant differences were observed at 73 and 81 dpi, triggering the ASO injections to be performed at 83-84 dpi (Figure 4C).

Consistent with our previous report[28], ASOs 2 and 3 were poorly tolerated at a pathological timepoint: 8/9 animals treated with active ASO 2 and 6/9 treated with control ASO 3 died or were euthanized 8-11 days post-surgery. In the active ASO 1 cohort, 2/9 animals also died 17-19 days post-surgery. Across treatment groups, all mice that survived the three-week period after surgery eventually developed progressive neurological signs consistent with prion disease, although half (9/18) of these mice, including N=3 saline-treated controls, did not reach terminal disease endpoint because they died acutely following intraperitoneal luciferin injection for live animal imaging (see Discussion).

Despite these complications, ASO 1 prolonged all-cause mortality by 46% (median 234 vs. 160 dpi; Figure 4D). Immediately after ICV injections, a sharp increase in BLI was observed in both saline- and ASO-treated mice, as a result of disease progression and/or inflammatory reaction to the surgical intervention (Figure 4D). BLI in mice treated with active ASO 1 declined to below the level in saline-treated animals at approximately three weeks post-dose, similar to time course at which NFL reversal was observed in the aforementioned experiment, albeit different ASOs were used (Figure 4A and 4C). Thereafter, BLI in saline-treated animals increased sharply up through terminal disease, while BLI in active ASO 1-treated animals remained low through terminal endpoint. In contrast to NfL, astrogliosis did not rebound at any timepoint after treatment, even as these mice developed typical prion disease on a similarly delayed schedule (medians 248 and 234 dpi in NfL and BLI experiments respectively, Figure 4B and 4D). These findings provide additional evidence that PrP-lowering can reverse pathological change.

Chronic dosing initiated at different timepoints

Antiprion compounds with non-PrP-lowering mechanisms of action have been most effective in prion-infected mice when administered prophylactically or very early after prion infection, with diminished or no efficacy as animals approached symptoms[29,32,62,63]. In ASO experiments described above and previously[28], we intervened at various timepoints, but comparison of efficacy between timepoints is complicated because these experiments also differed in their number of doses and in their experimental endpoints (symptomatic versus terminal disease). We therefore designed a controlled experiment to assess how timing of intervention impacts the efficacy of PrP-lowering therapy. We also employed a chronic dosing paradigm, to more closely approximate clinical use of existing ASO therapies. A total of N=112 mice were infected with RML prions and groups of N=8 received doses of 500 µg active ASO 6 or saline every 90 days beginning at -7, 1, 28, 54, 78, 105, or 120 dpi. Across timepoints, all mice in this experiment were followed to a symptomatic endpoint by blinded raters. This contrasts with our prior experiments, in which all late (83-129 dpi) treatment timepoints utilized a terminal endpoint (Fig 1, Table 2, Fig 4, ref. [28]).

Based on our natural history study, the first four timepoints in this experiment (-7 to 54 dpi) precede rise in plasma NfL. 78 dpi falls between the 60 dpi timepoint where some animals show initial NfL rise, and 90 dpi where plasma NfL elevation is consistently evident in prion-infected animals. The latest timepoints, 105 and 120 dpi, occur after NfL pathology is clearly detectable and around the time when symptomatic changes can begin to be detected.

Across the first five timepoints, including 78 dpi, (Figure 5A-E, Table S3), we observed a dramatic increase in time to symptomatic endpoint, driven both by an increase in healthy lifespan as well as by a slowing of initial symptomatic decline, as reflected in weights, symptoms, and nest-building (Figure S7A-C). Survival did not differ significantly between these five early timepoint groups (P = 0.29, Type I ANOVA, Figure 5A-E), although weight loss and nest-building defects, but not observable symptoms, appeared to be delayed somewhat longer in the

earliest-treated cohorts (Figure S7D-F). Initiation of treatment at later (105 and 120 dpi) timepoints, corresponding to 70% and 79% of the time to endpoint, still extended survival, although to a lesser extent compared to earlier timepoints (Figure 5F-G, Table S3). The effect size at 120 dpi observed in this experiment is smaller than our 120 dpi interventions against RML prions in which animals were followed to a terminal disease endpoint (Figure 1D and ref. [28]), and more similar to our result for 123 dpi intervention against RML prions with a symptomatic endpoint (Table 2), suggesting that different endpoints explain the different outcomes between experiments at this timepoint. Overall, late (105-120 dpi) treatment increased survival by 19% (median 175 dpi vs. 147 dpi across all saline controls; Figure 5H). Meanwhile early (≤78 dpi) initiation, when paired with chronic treatment, was able to drive a striking survival increase of about 3.0x (median 437 vs. 147 dpi across all saline controls), on par with the benefit we observed with genetic reduction of PrP in RML-infected heterozygous knockout mice (Figure 5H).

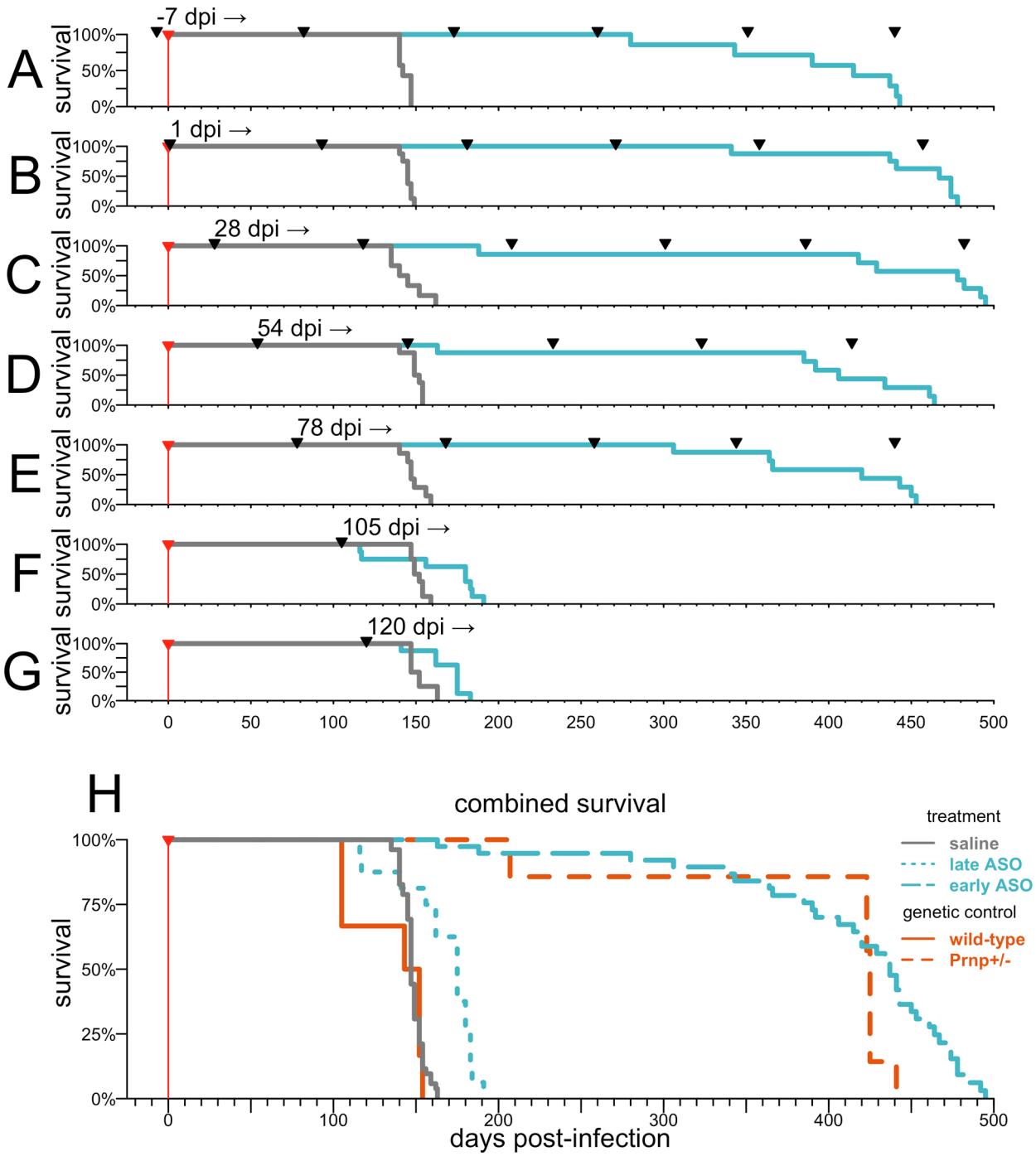

Figure 5. Efficacy of PrP-lowering therapy is timepoint-dependent. *Groups of N=8 animals received saline or active ASO 6, chronically every ~90 days beginning at the specified timepoint. Black triangle indicated when ASO was injected.* ***A-G)*** *Survival time as a function of time of treatment initiation,* ***H)*** *combined survival curves for saline-treated mice versus mice treated with active ASO 6 at early (-7 to 78 dpi) or late (105 to 120 dpi) timepoints. Survival curves for wild-type versus Prnp+/- animals infected with RML prions shown in Table 1 and Figure S3 are reproduced here for comparison. Studies conducted at the Broad Institute.*

Intervention at the symptomatic disease stage

In our natural history study, we observed suggestive or nominally significant group-wise differences between RML prion-infected and uninfected animals in terms of observation scores, rotarod performance, and nest-building by 120 dpi (Figure 3). This timepoint may, however, still precede the development of obvious individual symptoms in many animals (Figure S5, S6). We therefore undertook a series of later treatments overlapping the frankly symptomatic phase of RML prion disease. A total of N=96 mice were infected with RML prions, and groups of N=12 received a single dose of 500 µg active ASO 6 or saline at 120, 132, 143, or 156 dpi, and were followed to a terminal disease endpoint by blinded raters. As for previous experiments with a terminal endpoint (Figures 1, 4, and ref. [28]), treatment at 120 dpi extended survival of a majority of animals (Figure 6A), allowed some recovery of lost weight (Figure 6B) and attenuated symptom accumulation and loss of nest-building (Figure 6C-D).

By the 132 and 143 dpi timepoints, corresponding to 81% and 85% of the time to terminal endpoint, most or all (22/23 and 23/23 surviving animals, respectively) had already declined from their individual peak weights. By the 143 dpi timepoint, nest-building defects were also evident (Figure 6). At these timepoints, ASO treatment was effective in only a minority of animals. 35% of ASO-treated animals survived the immediate post-surgical period, living >10% (~17 days) longer than saline-treated controls. Those that did so lived considerably longer (mean 85 days), albeit without any measurable recovery in body weight or nest building (Figure 6E-L). By 156 dpi, when 7/23 (30%) of mice intended for treatment had already reached the terminal disease endpoint, PrP-lowering therapy had no effect (Figure 6M-P, Table S4).

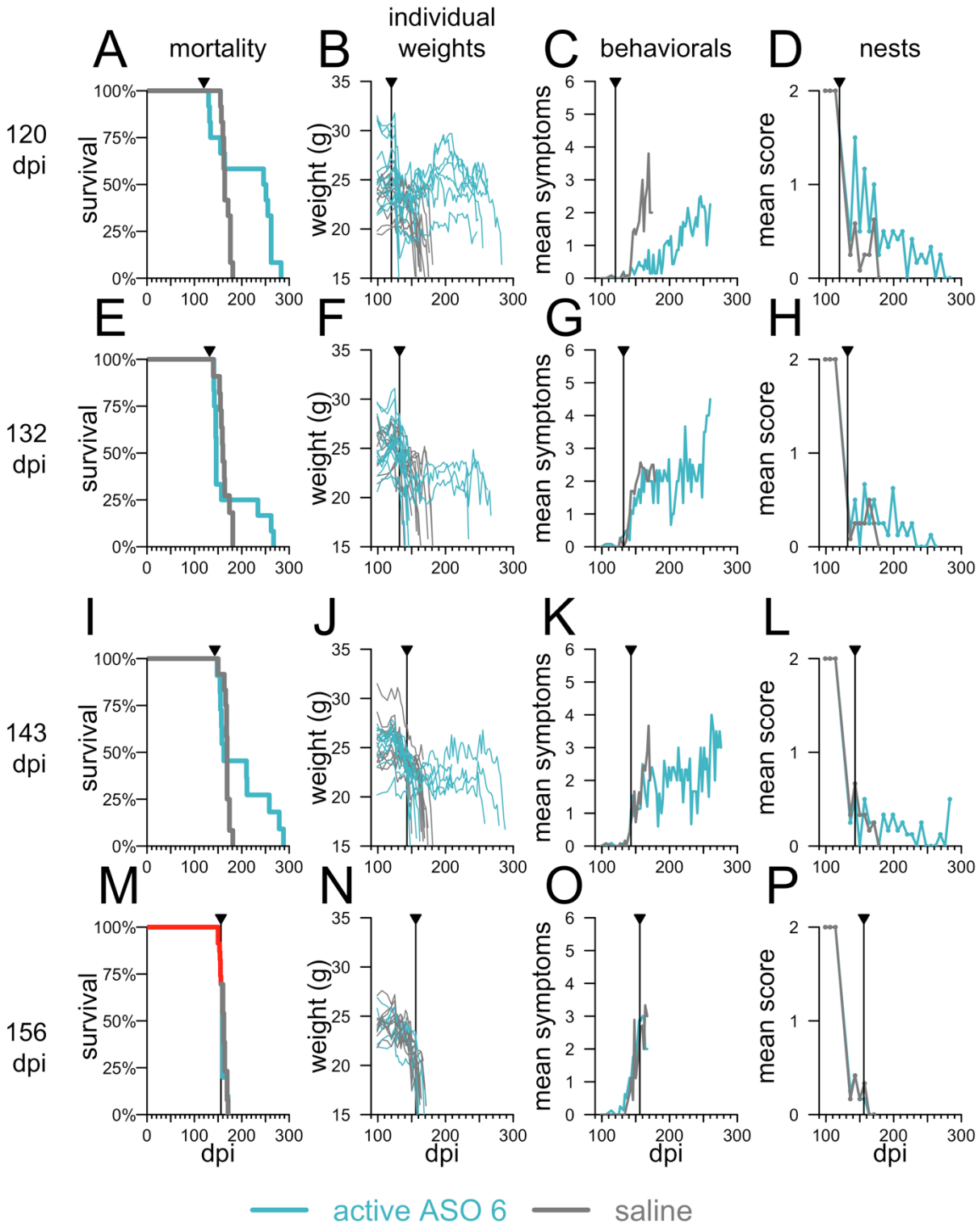

Figure 6. Effects of intervention at pathological and symptomatic timepoints. *Animals were infected with RML prions and then received saline (N=12) or a single 500 µg dose of active ASO 6 (N=12) at the indicated timepoint. A, E, I, M) survival; B, F, J, N) individual body weight trajectories; C, G, K, O) symptom count summarized by cohort; D, H, L, P) nest-building*

activity summarized by cohort. For the 156 dpi timepoint, 7/23 animals (30%) reached endpoint prior to the intervention (red curve, panel M). Studies conducted at the Broad Institute.

Discussion

PrP lowering is a longstanding therapeutic hypothesis. We recently reported that PrP-lowering ASOs are effective against prion disease. The present results expand on and broaden our previous findings, outlining the parameters that govern the efficacy of PrP-lowering therapies in prion disease.

We found that PrP-lowering ASOs extend survival in both prophylactic and delayed treatment paradigms, while non-PrP-targeting ASOs do not, replicating across ASO chemistries the reported efficacy and mechanism of action of ASOs in prion disease. In dose-response studies, we observed a clear relationship between degree of PrP suppression and extension of survival. Our experiments identified no minimum threshold to effect, with a clear survival benefit from even transient 21% knockdown, consistent with the continuous dose-response relationship postulated from genetic models[8]. Both pharmacologic and genetic reduction of PrP were substantially effective against five of five prion strains tested, and we did not observe emergence of drug resistance. This supports the universality of PrP lowering as a therapeutic strategy across strains and subtypes of prion disease. The above observations are also important because quantification of CSF PrP concentration[44,64,65] is being developed as a pharmacodynamic biomarker for PrP-lowering drugs. The validation of ASOs' mechanism of action *in vivo*, the tight relationship between degree of PrP lowering and disease delay, and the efficacy across prion strains, observed here all support the disease relevance of this biomarker[2].

The efficacy of previous antiprion therapies has depended critically upon the timepoint when treatment was initiated[29,32,62,63]. To better define disease timepoints in our animal model, we conducted natural history and biomarker studies in intracerebrally RML prion-inoculated mice. Biomarker evidence of pathology became clear well before the onset of detectable symptoms. Astrocytosis was detected by bioluminescence imaging beginning at 73-81 dpi, while plasma NfL became elevated in some animals by 60 and in all animals by 90 dpi. Notably, the disease-associated rise in both biomarkers could be measurably reversed by a single ASO treatment. In contrast, rotarod impairment became nominally detectable at 120 dpi, observable symptom profiles emerged by 116-135 dpi, and weight loss did not become obvious until 148 dpi. This is consistent with previous reports indicating neuroinflammatory changes can be observed by ~55-60 dpi[59,61,66], neuronal damage between 60-75 dpi[67], and behavioral or motor changes by ~105 dpi or later[66,68].

Overall, PrP-lowering therapy showed efficacy across a wide range of treatment timepoints. Chronic dosing initiated at pre-symptomatic timepoints up to early detectable pathology (≤78 dpi) tripled the time to a symptomatic endpoint (an increase of 290 days), both by extending healthy life and slowing initial decline. This matches the effect observed here and elsewhere[5–7] in heterozygous PrP knockout mice, and is consistent with PrP expression being required for both prion propagation and neurotoxicity[69,70]. Intervention at neuropathological timepoints approaching the time of earliest detectable symptomatic changes (83-120 dpi) also increased survival time, with reversal of neuronal damage and astrocytosis markers and some recovery of initial weight loss. At these pathological timepoints, we observed a modest delay (~1 month) in time to a symptomatic endpoint (accumulation of five prion disease symptoms), and a more profound delay (~3 months) in time to terminal disease (with criteria including 15-20% body weight loss). At frankly symptomatic timepoints (132-143 dpi), we observed a ~85 day delay in

terminal disease in approximately one third of animals (8/23), without reversal of weight loss, nesting, or symptomatic changes. At the most advanced symptomatic endpoint (156 dpi), no benefit was observed. This stage of disease may not allow not enough time for ASOs to take effect prior to animals reaching endpoint: although ASOs engage RNA targets within one week (Figure S1 and ref. [71]), our biomarker studies suggest a three-week lag time for this target engagement to impact established pathology (Figure 4). While the half-lives of PrP^{C} and PrP^{Sc} are reported to be on the order of 1-5 days[10,72], recovery from prion neurotoxicity may be more gradual. Broadly, the spectrum of outcomes observed at different timepoints may reflect accumulation of irreversible damage during the disease course, and may suggest the value of testing more aggressive dosing regimens when treatment is initiated later in the disease course.

Consistent with previous reports[22,28], not all preclinical ASOs were tolerated by mice with established prion neuropathology. This may reflect the minimal screening and optimization undertaken to identify these tool compounds. Studies to elucidate the mechanism of this phenomenon are ongoing. We also observed that animals with advanced prion disease often died immediately after luciferin injection for live animal imaging. Such deaths have not been reported before in Tg(*Gfa*p-luc) mice[60], have not been observed during our extensive experience of BLI studies in non-prion animals, and were never observed in our uninfected controls. Three saline-treated animals succumbed in this manner, ruling out a specific interaction between ASOs and luciferin, but instead suggesting the fragility of prion-infected mice to experimental manipulation.

Our study has important limitations. While we investigated two biomarkers and a large battery of symptom endpoints, our understanding of the natural history of experimental prion disease is by no means exhaustive, and other approaches have nominated putative pathological and symptomatic changes somewhat earlier than we observed here[59,66,68]. While we consistently observed an overall survival benefit to PrP-lowering therapy across nearly all paradigms tested, sometimes only a subset of mice benefitted, and the magnitude of therapeutic benefit observed sometimes varied between nearly identical experiments. This could reflect many contributing factors including variability in ICV dosing efficiency, human error in animal evaluation, and the imperfect tolerability of the ASO tool compounds employed.

Our findings provide basis for optimism that PrP lowering may be a promising therapeutic strategy, both for prophylaxis against prion disease onset in at-risk individuals with no evidence of disease process underway[43,44], and for treatment of active prion disease, during either prodromal or manifest disease. The effectiveness of a given PrP-lowering dosing regimen may vary depending on the stage of the disease, suggesting that dose regimens and trial endpoints may need to be adjusted depending on the clinical profile of the trial population.

Methods

Study design. At the Broad Institute, procedures (prion infection and ASO administration) were performed by investigators (SV and EVM) with full knowledge of study design, while all behavioral observations, weights, nest scores, and final endpoint determinations were taken by veterinary technicians (primarily JL and SG, with others on an on-call basis) blinded to the animals' treatment status or genotype. At the McLaughlin Research Institute, raters were not blinded. Disease endpoints (see below) were pre-specified at the time of protocol approval. All experiments were conducted under approved Institutional Animal Care and Use Committee protocols (Broad IACUC 0162-05-17, Ionis IACUC P-0273, and McLaughlin IACUC 2017-GAC22 / 2018-MPK29).

Animals. All studies used C57BL/6N female mice purchased from Charles River Laboratories or Taconic, except for the *Prnp*$^{+/-}$ mice[54] and wild-type controls (Table 1), which were C57BL/6N of both sexes, and the Tg(*Gfap*-luc) mice[60] (Figure 4), which are homozygous transgenics maintained on an FVB/N background at McLaughlin Research Institute.

Prion infection. Animals were infected at age 6-10 weeks by intracerebral prion inoculation with 30 µL of a 1% brain homogenate as described[28]. Briefly, brains were homogenized at 10% wt/vol in phosphate-buffered saline (Gibco 14190) in 7 mL tubes with zirconium oxide beads (Precellys no. KT039611307.7) using three 40 sec high pulses in a tissue homogenizer (Bertin EQ06404-200-RD000.0), diluted to 1% wt/vol, irradiated on dry ice at 7.0 kGy, extruded through progressively smaller-gauge blunt needles (Sai infusion B18, B21, B24, B27, B30), transferred to 2mL amber sealed sterile glass vials (Med Lab Supply), and then loaded into disposable syringes with 31G 6mm needles (BD SafetyGlide 328449). Animals were anesthetized with 3.0-3.5% isoflurane, received prophylactic meloxicam for analgesia and application of povidone/iodine as a disinfectant, and were freehand inoculated between the right ear and midline. The needle was withdrawn after three seconds and animals recovered from anesthesia in their home cages. Prion-infected brains for inoculation were supplied by co-investigators GAC (RML), KDH (Fukuoka-1 and 22L), HW, DM, and JA (ME7), and JYM (OSU). RML[ASO] brain homogenate was prepared from the pooled brains of three RML-infected animals that had received two 500 µg doses of active ASO 1 and succumbed to prion disease at 264, 270, and 270 dpi[28].

ASO administration. ASOs were administered into CSF by bolus stereotactic intracerebroventricular (ICV) injection as described[28]. Briefly, animals were anesthetized with 3.0-3.5% isoflurane, heads were shaved and swabbed with povidone/iodone, and prophylactic meloxicam analgesia was administered. Animals were placed in stereotaxis (ASI Instruments, SAS-4100), with 18° ear bars in ear canals and incisors in the mouse adapter tooth bar, adjusted to -8mm to level the bregma and lambda landmarks. Periosteum was scrubbed with sterile cotton-tipped applicators to reveal bregma following a ~1 cm scalp incision. Hamilton syringes (VWR 60376-172) fitted with 22-gauge Huber needles (VWR 82010-236) were filled with 10 µL of sterile saline (Gibco 14190) with or without ASO (diluted from 100 mg/mL). The needle was aligned to bregma and then moved 0.3 mm anterior, 1.0 mm right. The needle was then advanced ventral (downward) either 3.0 mm past where the bevel disappeared into the skull or 3.5 mm past where the tip of the needle first touched the skull. The liquid was ejected over ~10 seconds and the needle withdrawn 3 minutes later under downward pressure on the skull with a cotton-tipped applicator. Incisions were sutured (Ethicon 661H) with a horizontal mattress stitch. Animals recovered from the anesthesia in their home cages on a warming pad.

Neurofilament light quantification. Submandibular bleeds were collected with a 5mm sterile lancet (Braintree Scientific GR5MM) into a microtainer heparin blood tube (BD 365965). Tubes were inverted several times, placed on ice, and then spun at 6000 rpm for 12 min at 4°C. Plasma was transferred to a fresh cryotube and stored at -80°C until analysis. Plasma was diluted 1:4 with sample diluent and NfL was quantified using the Ella microfluidic ELISA platform (ProteinSimple) according to manufacturer's instructions.

Bioluminescence imaging. Each Tg(*Gfap*-luc) animal was given 5 mg (100 µL of 50 mg/mL) D-luciferin (GoldBio) in saline by intraperitoneal injection. After ~7 minutes to permit luciferin biodistribution plus ~7 minutes for 3.5% isoflurane induction, each animal was positioned into a Lumina II in vitro imaging system (IVIS; Perkin Elmer) with nosecone isoflurane maintenance and imagined for 1 minute before returning to its cage. At each session, three control Tg(*Gfap*-

luc) animals were imaged to test luciferin and equipment: two mice that received intraperitoneal lipopolysaccharide (LPS; positive control causing brain gliosis), and one mouse that received saline (negative control) 16h prior. Data for a single region of interest (ROI), defined based on an LPS positive control animal, were extracted using Living Image Software 4.5 (Perkin Elmer). Bioluminesence was measured in photons per second emitted from one square centimeter of tissue radiating into a solid angle of one steradian (sr) — photons/sec/cm^2/sr, also called radiance units or simply photons. This calibrated measure controls for charge coupled device (CCD) camera settings such as F-stop, exposure, and binning, in contrast with absolute measurement of incident photons, allowing adjustment of camera settings without compromising comparability of results.

qPCR. qPCR was performed as described[28] using primers *Prnp* forward: TCAGTCATCATGGCGAACCTT, reverse: AGGCCGACATCAGTCCACAT, and probe: CTACTGGCTGCTGGCCCTCTTTGTGACX; *Ppia* forward: TCGCCGCTTGCTGCA, reverse: ATCGGCCGTGATGTCGA, and probe: CCATGGTCAACCCCACCGTGTTCX. *Prnp* RNA levels were normalized to *Ppia* as a housekeeping gene and then to the mean of saline-treated controls.

Rotarod. Mice were seated on a rod rotating at 4 rpm in a 6-lane Rotarod apparatus (Maze Engineers). Once all mice from a single cage were properly seated, rotation was accelerated at 6 rotations per min for 5 min, and then held constant at 34 rpms for another 5 min. Latency to drop was recorded, in seconds, with a maximum score of 600 seconds if the mouse did not fall or ease itself off the rod. At each time point, the mice underwent 9 trials (3 trials per day over 3 days), with trials 1-3 considered to be spent learning the task and trials 4-9 included in analysis.

Disease monitoring and endpoints. At the Broad Institute, animals were checked for general healthy daily and subjected to detailed monitoring once weekly beginning at 90 dpi and thrice weekly beginning at 120 dpi. In these monitoring sessions, animals were weighed, and scored 0 or 1 for each of eight behavioral tests: scruff / poor grooming, poor body condition, reduced activity, hunched posture, irregular gait / hindlimb weakness, tremor, blank stare, and difficulty righting. Nest-building was rated for both cotton square nestlets (Ancare) and Enviro-dri® packed paper (Shepherd) on a scale of 0 = unused; 1 = used/pulled apart, but flat; 2 = pulled into a three-dimensional structure. Animals were euthanized by CO_2 inhalation when they met pre-defined endpoint criteria. Terminal endpoint criteria, intended to catch mice just shortly before disease progressed naturally to death, were defined initially as body condition score <2, body weight loss ≥20% from baseline, inability to reach food or water, severe respiratory distress, or severe neurological deficits (Figure 1D-F), and later refined to simply body weight loss ≥15% from baseline or inability to reach food or water (Figure 6). Symptomatic endpoint criteria, intended to catch mice at an advanced disease stage but before terminal illness, were defined as ≥5 of the 8 pre-defined symptoms being observed at two consecutive monitoring sessions, or body weight loss ≥15% from baseline, body condition score ≤2, or inability to reach food or water (Figures 2 and 5 and Tables 1 and 2). At the McLaughlin Research Institute, mice were monitored for diverse neurological and non-neurological health indicators and SHIRPA phenotypes[73] (Table S2) in the natural history study (Figure 3), and checked for general health and weight in other studies (Figure 4); they were euthanized at ≥20% body weight loss from baseline, inability to reach food or water, or moribund status.

Statistical analysis. Most differences in outcomes were considered visually obvious and were not subjected to statistical tests. Statistical tests, where performed, were two-sided and are named throughout the text, with all reported *P* values being nominal. To avoid selective reporting of only those deaths subjectively attributed to prion disease, survival curves reported

herein include all causes of death except for the following: death prior to any drug treatment (meaning prior to experimental treatment group being assigned); acute deaths within 1 day post-surgery due to surgical complications; and euthanasia due to experimental error (such as incorrect dosing or inability to position animal in stereotaxis).

Data availability. Individual-level data for every experimental animal are provided in a public repository along with R source code sufficient to reproduce all of the figures and tables in this manuscript: https://github.com/ericminikel/prp_lowering

Acknowledgements

We thank Rob Pulido, Cecilia Monteiro, Anne Smith, and Tiffany Baumann for critical review of the manuscript, Karli Ikeda-Lee and Amanda Sevilleja for technical assistance, Johnnatan Tamayo and Donna Sipe for vivarium assistance. Studies at the Broad Institute were supported by the Broad Next Gen Fund, Prion Alliance, direct donations to Prions@Broad, the National Institutes of Health (F31 AI122592 to EVM), the National Science Foundation (GRFP 2015214731 to SV), and an anonymous organization. Studies at McLaughlin Research Institute were supported by Prion Alliance and Ionis Pharmaceuticals. Studies at Ionis Pharmaceuticals were funded by Ionis Pharmaceuticals.

Declaration of interests

SMV has received speaking fees from Illumina and Biogen and has received research support in the form of unrestricted charitable contributions from Charles River Laboratories and Ionis Pharmaceuticals. EVM has received consulting fees from Deerfield Management and Guidepoint and has received research support in the form of unrestricted charitable contributions from Charles River Laboratories and Ionis Pharmaceuticals. HTZ and HBK are employees and shareholders of Ionis Pharmaceuticals. DEC has received research support from Ionis Pharmaceuticals. JBC has received research support from Ionis Pharmaceuticals, Wave Life Sciences, Triplet Therapeutics and consulting fees from Skyhawk Therapeutics and Guidepoint. SLS serves on the Board of Directors of the Genomics Institute of the Novartis Research Foundation (“GNF”); is a shareholder and serves on the Board of Directors of Jnana Therapeutics; is a shareholder of Forma Therapeutics; is a shareholder and advises Kojin Therapeutics, Kisbee Therapeutics, Decibel Therapeutics and Eikonizo Therapeutics; serves on the Scientific Advisory Boards of Eisai Co., Ltd., Ono Pharma Foundation, Exo Therapeutics, and F-Prime Capital Partners; and is a Novartis Faculty Scholar. Other authors report no conflicts.

Author contributions

Conceived and designed the studies: SMV, DEC, HBK, HTZ, EVM, JBC, GAC
Analyzed the data: EVM, SMV, HTZ, DEC, JBK
Provided key methods or reagents: GAC, JK, JBK, JYM, HW, DM, JA, KDH
Performed the experiments: SMV, DEC, HTZ, EVM, JL, JOM, RP, SG
Supervised the research: SMV, DEC, HBK, TC, JS, MB, SLS, ROK
Wrote the manuscript: SMV, EVM, HTZ, HBK, DEC
Reviewed, edited and approved the final manuscript: All authors

References

1. Prusiner SB. Prions. Proc Natl Acad Sci USA. 1998 Nov 10;95(23):13363–13383. PMCID: PMC33918
2. Vallabh SM, Minikel EV, Schreiber SL, Lander ES. Towards a treatment for genetic prion disease: trials and biomarkers. The Lancet Neurology. 2020;19(4):361–368.
3. Büeler H, Aguzzi A, Sailer A, Greiner RA, Autenried P, Aguet M, Weissmann C. Mice devoid of PrP are resistant to scrapie. Cell. 1993 Jul 2;73(7):1339–1347. PMID: 8100741
4. Salvesen Ø, Espenes A, Reiten MR, Vuong TT, Malachin G, Tran L, Andréoletti O, Olsaker I, Benestad SL, Tranulis MA, Ersdal C. Goats naturally devoid of PrPC are resistant to scrapie. Vet Res. 2020 Jan 10;51(1):1. PMCID: PMC6954626
5. Büeler H, Raeber A, Sailer A, Fischer M, Aguzzi A, Weissmann C. High prion and PrPSc levels but delayed onset of disease in scrapie-inoculated mice heterozygous for a disrupted PrP gene. Mol Med. 1994 Nov;1(1):19–30. PMCID: PMC2229922
6. Prusiner SB, Groth D, Serban A, Koehler R, Foster D, Torchia M, Burton D, Yang SL, DeArmond SJ. Ablation of the prion protein (PrP) gene in mice prevents scrapie and facilitates production of anti-PrP antibodies. Proc Natl Acad Sci USA. 1993 Nov 15;90(22):10608–10612. PMCID: PMC47826
7. Sakaguchi S, Katamine S, Shigematsu K, Nakatani A, Moriuchi R, Nishida N, Kurokawa K, Nakaoke R, Sato H, Jishage K. Accumulation of proteinase K-resistant prion protein (PrP) is restricted by the expression level of normal PrP in mice inoculated with a mouse-adapted strain of the Creutzfeldt-Jakob disease agent. J Virol. 1995 Dec;69(12):7586–7592. PMCID: PMC189697
8. Fischer M, Rülicke T, Raeber A, Sailer A, Moser M, Oesch B, Brandner S, Aguzzi A, Weissmann C. Prion protein (PrP) with amino-proximal deletions restoring susceptibility of PrP knockout mice to scrapie. EMBO J. 1996 Mar 15;15(6):1255–1264. PMCID: PMC450028
9. Mallucci G, Dickinson A, Linehan J, Klöhn P-C, Brandner S, Collinge J. Depleting neuronal PrP in prion infection prevents disease and reverses spongiosis. Science. 2003 Oct 31;302(5646):871–874. PMID: 14593181
10. Safar JG, DeArmond SJ, Kociuba K, Deering C, Didorenko S, Bouzamondo-Bernstein E, Prusiner SB, Tremblay P. Prion clearance in bigenic mice. J Gen Virol. 2005 Oct;86(Pt 10):2913–2923. PMID: 16186247
11. Büeler H, Fischer M, Lang Y, Bluethmann H, Lipp HP, DeArmond SJ, Prusiner SB, Aguet M, Weissmann C. Normal development and behaviour of mice lacking the neuronal cell-surface PrP protein. Nature. 1992 Apr 16;356(6370):577–582. PMID: 1373228
12. Richt JA, Kasinathan P, Hamir AN, Castilla J, Sathiyaseelan T, Vargas F, Sathiyaseelan J, Wu H, Matsushita H, Koster J, Kato S, Ishida I, Soto C, Robl JM, Kuroiwa Y. Production of cattle lacking prion protein. Nat Biotechnol. 2007 Jan;25(1):132–138. PMCID: PMC2813193
13. Benestad SL, Austbø L, Tranulis MA, Espenes A, Olsaker I. Healthy goats naturally devoid of prion protein. Vet Res. 2012;43:87. PMCID: PMC3542104
14. Küffer A, Lakkaraju AKK, Mogha A, Petersen SC, Airich K, Doucerain C, Marpakwar R, Bakirci P, Senatore A, Monnard A, Schiavi C, Nuvolone M, Grosshans B, Hornemann S, Bassilana F, Monk KR, Aguzzi A. The prion protein is an agonistic ligand of the G protein-coupled receptor Adgrg6. Nature. 2016 Aug 25;536(7617):464–468. PMID: 27501152

15. Bremer J, Baumann F, Tiberi C, Wessig C, Fischer H, Schwarz P, Steele AD, Toyka KV, Nave K-A, Weis J, Aguzzi A. Axonal prion protein is required for peripheral myelin maintenance. Nat Neurosci. 2010 Mar;13(3):310–318. PMID: 20098419
16. Skedsmo FS, Malachin G, Våge DI, Hammervold MM, Salvesen Ø, Ersdal C, Ranheim B, Stafsnes MH, Bartosova Z, Bruheim P, Jäderlund KH, Matiasek K, Espenes A, Tranulis MA. Demyelinating polyneuropathy in goats lacking prion protein. FASEB J. 2019 Dec 13; PMID: 31907995
17. Minikel EV, Vallabh SM, Lek M, Estrada K, Samocha KE, Sathirapongsasuti JF, McLean CY, Tung JY, Yu LPC, Gambetti P, Blevins J, Zhang S, Cohen Y, Chen W, Yamada M, Hamaguchi T, Sanjo N, Mizusawa H, Nakamura Y, Kitamoto T, Collins SJ, Boyd A, Will RG, Knight R, Ponto C, Zerr I, Kraus TFJ, Eigenbrod S, Giese A, Calero M, de Pedro-Cuesta J, Haïk S, Laplanche J-L, Bouaziz-Amar E, Brandel J-P, Capellari S, Parchi P, Poleggi A, Ladogana A, O'Donnell-Luria AH, Karczewski KJ, Marshall JL, Boehnke M, Laakso M, Mohlke KL, Kähler A, Chambert K, McCarroll S, Sullivan PF, Hultman CM, Purcell SM, Sklar P, van der Lee SJ, Rozemuller A, Jansen C, Hofman A, Kraaij R, van Rooij JGJ, Ikram MA, Uitterlinden AG, van Duijn CM, Exome Aggregation Consortium (ExAC), Daly MJ, MacArthur DG. Quantifying prion disease penetrance using large population control cohorts. Sci Transl Med. 2016 Jan 20;8(322):322ra9. PMCID: PMC4774245
18. Minikel EV, Karczewski KJ, Martin HC, Cummings BB, Whiffin N, Alfoldi J, Trembath RC, van Heel DA, Daly MJ, Schreiber SL, MacArthur DG. Evaluating drug targets through human loss-of-function genetic variation. bioRxiv. 2019 Jan 29;530881.
19. Lledo PM, Tremblay P, DeArmond SJ, Prusiner SB, Nicoll RA. Mice deficient for prion protein exhibit normal neuronal excitability and synaptic transmission in the hippocampus. Proc Natl Acad Sci USA. 1996 Mar 19;93(6):2403–2407. PMCID: PMC39809
20. White MD, Farmer M, Mirabile I, Brandner S, Collinge J, Mallucci GR. Single treatment with RNAi against prion protein rescues early neuronal dysfunction and prolongs survival in mice with prion disease. Proc Natl Acad Sci USA. 2008 Jul 22;105(29):10238–10243. PMCID: PMC2474561
21. Pulford B, Reim N, Bell A, Veatch J, Forster G, Bender H, Meyerett C, Hafeman S, Michel B, Johnson T, Wyckoff AC, Miele G, Julius C, Kranich J, Schenkel A, Dow S, Zabel MD. Liposome-siRNA-peptide complexes cross the blood-brain barrier and significantly decrease PrP on neuronal cells and PrP in infected cell cultures. PLoS ONE. 2010;5(6):e11085. PMCID: PMC2885418
22. Nazor Friberg K, Hung G, Wancewicz E, Giles K, Black C, Freier S, Bennett F, Dearmond SJ, Freyman Y, Lessard P, Ghaemmaghami S, Prusiner SB. Intracerebral Infusion of Antisense Oligonucleotides Into Prion-infected Mice. Mol Ther Nucleic Acids. 2012;1:e9. PMCID: PMC3381600
23. Ahn M, Bajsarowicz K, Oehler A, Lemus A, Bankiewicz K, DeArmond SJ. Convection-enhanced delivery of AAV2-PrPshRNA in prion-infected mice. PLoS ONE. 2014;9(5):e98496. PMCID: PMC4035323
24. Lehmann S, Relano-Gines A, Resina S, Brillaud E, Casanova D, Vincent C, Hamela C, Poupeau S, Laffont M, Gabelle A, Delaby C, Belondrade M, Arnaud J-D, Alvarez M-T, Maurel J-C, Maurel P, Crozet C. Systemic delivery of siRNA down regulates brain prion protein and ameliorates neuropathology in prion disorder. PLoS ONE. 2014;9(2):e88797. PMCID: PMC3925167
25. Tabrizi SJ, Leavitt BR, Landwehrmeyer GB, Wild EJ, Saft C, Barker RA, Blair NF, Craufurd D, Priller J, Rickards H, Rosser A, Kordasiewicz HB, Czech C, Swayze EE, Norris DA, Baumann T, Gerlach I, Schobel SA, Paz E, Smith AV, Bennett CF, Lane RM.

Targeting Huntingtin Expression in Patients with Huntington's Disease. N Engl J Med. 2019 May 6; PMID: 31059641

26. Miller TM, Cudkowicz ME, Shaw PJ, Graham D, Fradette S, Houshyar H, Bennett F, Lane RM, Nestorov I, Fanning L, others. Safety, PK, PD, and exploratory efficacy in a single and multiple-dose study of a SOD1 antisense oligonucleotide (BIIB067) administered to participants with ALS. Neurology. Philadelphia, PA; 2019. p. E533–E533.
27. Bennett CF. Therapeutic Antisense Oligonucleotides Are Coming of Age. Annu Rev Med. 2019 Jan 27;70:307–321. PMID: 30691367
28. Raymond GJ, Zhao HT, Race B, Raymond LD, Williams K, Swayze EE, Graffam S, Le J, Caron T, Stathopoulos J, O'Keefe R, Lubke LL, Reidenbach AG, Kraus A, Schreiber SL, Mazur C, Cabin DE, Carroll JB, Minikel EV, Kordasiewicz H, Caughey B, Vallabh SM. Antisense oligonucleotides extend survival of prion-infected mice. JCI Insight. 2019 30;5. PMID: 31361599
29. Kawasaki Y, Kawagoe K, Chen C, Teruya K, Sakasegawa Y, Doh-ura K. Orally administered amyloidophilic compound is effective in prolonging the incubation periods of animals cerebrally infected with prion diseases in a prion strain-dependent manner. J Virol. 2007 Dec;81(23):12889–12898. PMCID: PMC2169081
30. Berry DB, Lu D, Geva M, Watts JC, Bhardwaj S, Oehler A, Renslo AR, DeArmond SJ, Prusiner SB, Giles K. Drug resistance confounding prion therapeutics. Proc Natl Acad Sci USA. 2013 Oct 29;110(44):E4160-4169. PMCID: PMC3816483
31. Lu D, Giles K, Li Z, Rao S, Dolghih E, Gever JR, Geva M, Elepano ML, Oehler A, Bryant C, Renslo AR, Jacobson MP, Dearmond SJ, Silber BM, Prusiner SB. Biaryl amides and hydrazones as therapeutics for prion disease in transgenic mice. J Pharmacol Exp Ther. 2013 Nov;347(2):325–338. PMCID: PMC3807058
32. Giles K, Berry DB, Condello C, Hawley RC, Gallardo-Godoy A, Bryant C, Oehler A, Elepano M, Bhardwaj S, Patel S, Silber BM, Guan S, DeArmond SJ, Renslo AR, Prusiner SB. Different 2-Aminothiazole Therapeutics Produce Distinct Patterns of Scrapie Prion Neuropathology in Mouse Brains. J Pharmacol Exp Ther. 2015 Oct;355(1):2–12. PMID: 26224882
33. Giles K, Berry DB, Condello C, Dugger BN, Li Z, Oehler A, Bhardwaj S, Elepano M, Guan S, Silber BM, Olson SH, Prusiner SB. Optimization of Aryl Amides that Extend Survival in Prion-Infected Mice. J Pharmacol Exp Ther. 2016 Sep;358(3):537–547. PMCID: PMC4998675
34. Ghaemmaghami S, Ahn M, Lessard P, Giles K, Legname G, DeArmond SJ, Prusiner SB. Continuous quinacrine treatment results in the formation of drug-resistant prions. PLoS Pathog. 2009 Nov;5(11):e1000673. PMCID: PMC2777304
35. Li J, Browning S, Mahal SP, Oelschlegel AM, Weissmann C. Darwinian evolution of prions in cell culture. Science. 2010 Feb 12;327(5967):869–872. PMCID: PMC2848070
36. Pocchiari M, Puopolo M, Croes EA, Budka H, Gelpi E, Collins S, Lewis V, Sutcliffe T, Guilivi A, Delasnerie-Laupretre N, Brandel J-P, Alperovitch A, Zerr I, Poser S, Kretzschmar HA, Ladogana A, Rietvald I, Mitrova E, Martinez-Martin P, de Pedro-Cuesta J, Glatzel M, Aguzzi A, Cooper S, Mackenzie J, van Duijn CM, Will RG. Predictors of survival in sporadic Creutzfeldt-Jakob disease and other human transmissible spongiform encephalopathies. Brain. 2004 Oct;127(Pt 10):2348–2359. PMID: 15361416
37. Groveman BR, Orrú CD, Hughson AG, Bongianni M, Fiorini M, Imperiale D, Ladogana A, Pocchiari M, Zanusso G, Caughey B. Extended and direct evaluation of RT-QuIC assays for Creutzfeldt-Jakob disease diagnosis. Ann Clin Transl Neurol. 2017 Feb;4(2):139–144. PMCID: PMC5288466
38. Franceschini A, Baiardi S, Hughson AG, McKenzie N, Moda F, Rossi M, Capellari S, Green A, Giaccone G, Caughey B, Parchi P. High diagnostic value of second generation

CSF RT-QuIC across the wide spectrum of CJD prions. Sci Rep. 2017 Sep 6;7(1):10655. PMCID: PMC5587608

39. Abu-Rumeileh S, Capellari S, Stanzani-Maserati M, Polischi B, Martinelli P, Caroppo P, Ladogana A, Parchi P. The CSF neurofilament light signature in rapidly progressive neurodegenerative dementias. Alzheimers Res Ther. 2018 Jan 11;10(1):3. PMCID: PMC5784714
40. Thompson AGB, Luk C, Heslegrave AJ, Zetterberg H, Mead SH, Collinge J, Jackson GS. Neurofilament light chain and tau concentrations are markedly increased in the serum of patients with sporadic Creutzfeldt-Jakob disease, and tau correlates with rate of disease progression. J Neurol Neurosurg Psychiatry. 2018 Sep;89(9):955–961. PMCID: PMC6109239
41. Staffaroni AM, Kramer AO, Casey M, Kang H, Rojas JC, Orrú CD, Caughey B, Allen IE, Kramer JH, Rosen HJ, Blennow K, Zetterberg H, Geschwind MD. Association of Blood and Cerebrospinal Fluid Tau Level and Other Biomarkers With Survival Time in Sporadic Creutzfeldt-Jakob Disease. JAMA Neurol. 2019 May 6; PMCID: PMC6503575
42. Foutz A, Appleby BS, Hamlin C, Liu X, Yang S, Cohen Y, Chen W, Blevins J, Fausett C, Wang H, Gambetti P, Zhang S, Hughson A, Tatsuoka C, Schonberger LB, Cohen ML, Caughey B, Safar JG. Diagnostic and prognostic value of human prion detection in cerebrospinal fluid. Ann Neurol. 2017 Jan;81(1):79–92. PMCID: PMC5266667
43. Minikel EV, Vallabh SM, Orseth MC, Brandel J-P, Haïk S, Laplanche J-L, Zerr I, Parchi P, Capellari S, Safar J, Kenny J, Fong JC, Takada LT, Ponto C, Hermann P, Knipper T, Stehmann C, Kitamoto T, Ae R, Hamaguchi T, Sanjo N, Tsukamoto T, Mizusawa H, Collins SJ, Chiesa R, Roiter I, de Pedro-Cuesta J, Calero M, Geschwind MD, Yamada M, Nakamura Y, Mead S. Age at onset in genetic prion disease and the design of preventive clinical trials. Neurology. 2019 Jun 6; PMID: 31171647
44. Vallabh SM, Minikel EV, Williams VJ, Carlyle BC, McManus AJ, Wennick CD, Bolling A, Trombetta BA, Urick D, Nobuhara CK, Gerber J, Duddy H, Lachmann I, Stehmann C, Collins SJ, Blennow K, Zetterberg H, Arnold SE. Cerebrospinal fluid and plasma biomarkers in individuals at risk for genetic prion disease. medRxiv. 2019 Dec 15;2019.12.13.19014217.
45. Bennett CF, Baker BF, Pham N, Swayze E, Geary RS. Pharmacology of Antisense Drugs. Annu Rev Pharmacol Toxicol. 2017 Jan 6;57:81–105. PMID: 27732800
46. McCampbell A, Cole T, Wegener AJ, Tomassy GS, Setnicka A, Farley BJ, Schoch KM, Hoye ML, Shabsovich M, Sun L, Luo Y, Zhang M, Thankamony S, Salzman DW, Cudkowicz M, Graham DL, Bennett CF, Kordasiewicz HB, Swayze EE, Miller TM, Comfort N, Wang B, Amacker J. Antisense oligonucleotides extend survival and reverse decrement in muscle response in ALS models. J Clin Invest. 2018 01;128(8):3558–3567. PMCID: PMC6063493
47. Chandler RL. Encephalopathy in mice produced by inoculation with scrapie brain material. Lancet. 1961 Jun 24;1(7191):1378–1379. PMID: 13692303
48. Watts JC, Prusiner SB. Mouse models for studying the formation and propagation of prions. J Biol Chem. 2014 Jul 18;289(29):19841–19849. PMCID: PMC4106304
49. Reidenbach AG, Minikel EV, Zhao HT, Guzman SG, Leed AJ, Mesleh MF, Kordasiewicz HB, Schreiber SL, Vallabh SM. Characterization of the Prion Protein Binding Properties of Antisense Oligonucleotides. Biomolecules. 2019 Dec 18;10(1). PMID: 31861275
50. Bruce ME, McConnell I, Fraser H, Dickinson AG. The disease characteristics of different strains of scrapie in Sinc congenic mouse lines: implications for the nature of the agent and host control of pathogenesis. J Gen Virol. 1991 Mar;72 (Pt 3):595–603. PMID: 1672371

51. Zlotnik I, Rennie JC. Further observations on the experimental transmission of scrapie from sheep and goats to laboratory mice. J Comp Pathol. 1963 Apr;73:150–162. PMID: 14003830
52. Tateishi J, Kitamoto T. Inherited prion diseases and transmission to rodents. Brain Pathol. 1995 Jan;5(1):53–59. PMID: 7767491
53. Wang F, Wang X, Yuan C-G, Ma J. Generating a prion with bacterially expressed recombinant prion protein. Science. 2010 Feb 26;327(5969):1132–1135. PMCID: PMC2893558
54. Nuvolone M, Hermann M, Sorce S, Russo G, Tiberi C, Schwarz P, Minikel E, Sanoudou D, Pelczar P, Aguzzi A. Strictly co-isogenic C57BL/6J-Prnp-/- mice: A rigorous resource for prion science. J Exp Med. 2016 Mar 7;213(3):313–327. PMCID: PMC4813672
55. Herrmann US, Schütz AK, Shirani H, Huang D, Saban D, Nuvolone M, Li B, Ballmer B, Åslund AKO, Mason JJ, Rushing E, Budka H, Nyström S, Hammarström P, Böckmann A, Caflisch A, Meier BH, Nilsson KPR, Hornemann S, Aguzzi A. Structure-based drug design identifies polythiophenes as antiprion compounds. Sci Transl Med. 2015 Aug 5;7(299):299ra123. PMID: 26246168
56. Bacioglu M, Maia LF, Preische O, Schelle J, Apel A, Kaeser SA, Schweighauser M, Eninger T, Lambert M, Pilotto A, Shimshek DR, Neumann U, Kahle PJ, Staufenbiel M, Neumann M, Maetzler W, Kuhle J, Jucker M. Neurofilament Light Chain in Blood and CSF as Marker of Disease Progression in Mouse Models and in Neurodegenerative Diseases. Neuron. 2016 06;91(1):56–66. PMID: 27292537
57. Byrne LM, Rodrigues FB, Blennow K, Durr A, Leavitt BR, Roos RAC, Scahill RI, Tabrizi SJ, Zetterberg H, Langbehn D, Wild EJ. Neurofilament light protein in blood as a potential biomarker of neurodegeneration in Huntington's disease: a retrospective cohort analysis. Lancet Neurol. 2017;16(8):601–609. PMCID: PMC5507767
58. Preische O, Schultz SA, Apel A, Kuhle J, Kaeser SA, Barro C, Gräber S, Kuder-Buletta E, LaFougere C, Laske C, Vöglein J, Levin J, Masters CL, Martins R, Schofield PR, Rossor MN, Graff-Radford NR, Salloway S, Ghetti B, Ringman JM, Noble JM, Chhatwal J, Goate AM, Benzinger TLS, Morris JC, Bateman RJ, Wang G, Fagan AM, McDade EM, Gordon BA, Jucker M, Dominantly Inherited Alzheimer Network. Serum neurofilament dynamics predicts neurodegeneration and clinical progression in presymptomatic Alzheimer's disease. Nat Med. 2019;25(2):277–283. PMCID: PMC6367005
59. Hwang D, Lee IY, Yoo H, Gehlenborg N, Cho J-H, Petritis B, Baxter D, Pitstick R, Young R, Spicer D, Price ND, Hohmann JG, Dearmond SJ, Carlson GA, Hood LE. A systems approach to prion disease. Mol Syst Biol. 2009;5:252. PMCID: PMC2671916
60. Zhu L, Ramboz S, Hewitt D, Boring L, Grass DS, Purchio AF. Non-invasive imaging of GFAP expression after neuronal damage in mice. Neurosci Lett. 2004 Sep 2;367(2):210–212. PMID: 15331155
61. Tamgüney G, Francis KP, Giles K, Lemus A, DeArmond SJ, Prusiner SB. Measuring prions by bioluminescence imaging. Proc Natl Acad Sci USA. 2009 Sep 1;106(35):15002–15006. PMCID: PMC2736416
62. Doh-ura K, Ishikawa K, Murakami-Kubo I, Sasaki K, Mohri S, Race R, Iwaki T. Treatment of transmissible spongiform encephalopathy by intraventricular drug infusion in animal models. J Virol. 2004 May;78(10):4999–5006. PMCID: PMC400350
63. Wagner J, Ryazanov S, Leonov A, Levin J, Shi S, Schmidt F, Prix C, Pan-Montojo F, Bertsch U, Mitteregger-Kretzschmar G, Geissen M, Eiden M, Leidel F, Hirschberger T, Deeg AA, Krauth JJ, Zinth W, Tavan P, Pilger J, Zweckstetter M, Frank T, Bähr M, Weishaupt JH, Uhr M, Urlaub H, Teichmann U, Samwer M, Bötzel K, Groschup M, Kretzschmar H, Griesinger C, Giese A. Anle138b: a novel oligomer modulator for disease-modifying therapy of neurodegenerative diseases such as prion and Parkinson's disease. Acta Neuropathol. 2013 Jun;125(6):795–813. PMCID: PMC3661926

64. Vallabh SM, Nobuhara CK, Llorens F, Zerr I, Parchi P, Capellari S, Kuhn E, Klickstein J, Safar JG, Nery FC, Swoboda KJ, Geschwind MD, Zetterberg H, Arnold SE, Minikel EV, Schreiber SL. Prion protein quantification in human cerebrospinal fluid as a tool for prion disease drug development. PNAS. 2019 Apr 1;201901947. PMID: 30936307
65. Minikel EV, Kuhn E, Cocco AR, Vallabh SM, Hartigan CR, Reidenbach AG, Safar JG, Raymond GJ, McCarthy MD, O'Keefe R, Llorens F, Zerr I, Capellari S, Parchi P, Schreiber SL, Carr SA. Domain-specific quantification of prion protein in cerebrospinal fluid by targeted mass spectrometry. Mol Cell Proteomics. 2019 Sep 26; PMID: 31558565
66. Sorce S, Nuvolone M, Russo G, Chincisan A, Heinzer D, Avar M, Pfammatter M, Schwarz P, Delic M, Hornemann S, Sanoudou D, Scheckel C, Aguzzi A. Genome-wide transcriptomics identifies an early preclinical signature of prion infection. bioRxiv. 2020 Jan 11;2020.01.10.901637.
67. Hirouchi M. Neurofilament light chain (NfL) as a possible biomarker for drug efficacy in mouse models of neurodegenerative diseases [Internet]. Prion2019; 2019 May 21; Edmonton, AB. Available from: https://www.ncbi.nlm.nih.gov/pmc/articles/PMC6738495/
68. Steele AD, Jackson WS, King OD, Lindquist S. The power of automated high-resolution behavior analysis revealed by its application to mouse models of Huntington's and prion diseases. Proc Natl Acad Sci USA. 2007 Feb 6;104(6):1983–1988. PMCID: PMC1794260
69. Brandner S, Isenmann S, Raeber A, Fischer M, Sailer A, Kobayashi Y, Marino S, Weissmann C, Aguzzi A. Normal host prion protein necessary for scrapie-induced neurotoxicity. Nature. 1996 Jan 25;379(6563):339–343. PMID: 8552188
70. Sandberg MK, Al-Doujaily H, Sharps B, De Oliveira MW, Schmidt C, Richard-Londt A, Lyall S, Linehan JM, Brandner S, Wadsworth JDF, Clarke AR, Collinge J. Prion neuropathology follows the accumulation of alternate prion protein isoforms after infective titre has peaked. Nat Commun. 2014 Jul 9;5:4347. PMCID: PMC4104459
71. Rigo F, Chun SJ, Norris DA, Hung G, Lee S, Matson J, Fey RA, Gaus H, Hua Y, Grundy JS, Krainer AR, Henry SP, Bennett CF. Pharmacology of a central nervous system delivered 2'-O-methoxyethyl-modified survival of motor neuron splicing oligonucleotide in mice and nonhuman primates. J Pharmacol Exp Ther. 2014 Jul;350(1):46–55. PMCID: PMC4056267
72. Price JC, Guan S, Burlingame A, Prusiner SB, Ghaemmaghami S. Analysis of proteome dynamics in the mouse brain. Proc Natl Acad Sci USA. 2010 Aug 10;107(32):14508–14513. PMCID: PMC2922600
73. Rogers DC, Fisher EM, Brown SD, Peters J, Hunter AJ, Martin JE. Behavioral and functional analysis of mouse phenotype: SHIRPA, a proposed protocol for comprehensive phenotype assessment. Mamm Genome. 1997 Oct;8(10):711–713. PMID: 9321461

SUPPLEMENTARY MATERIALS

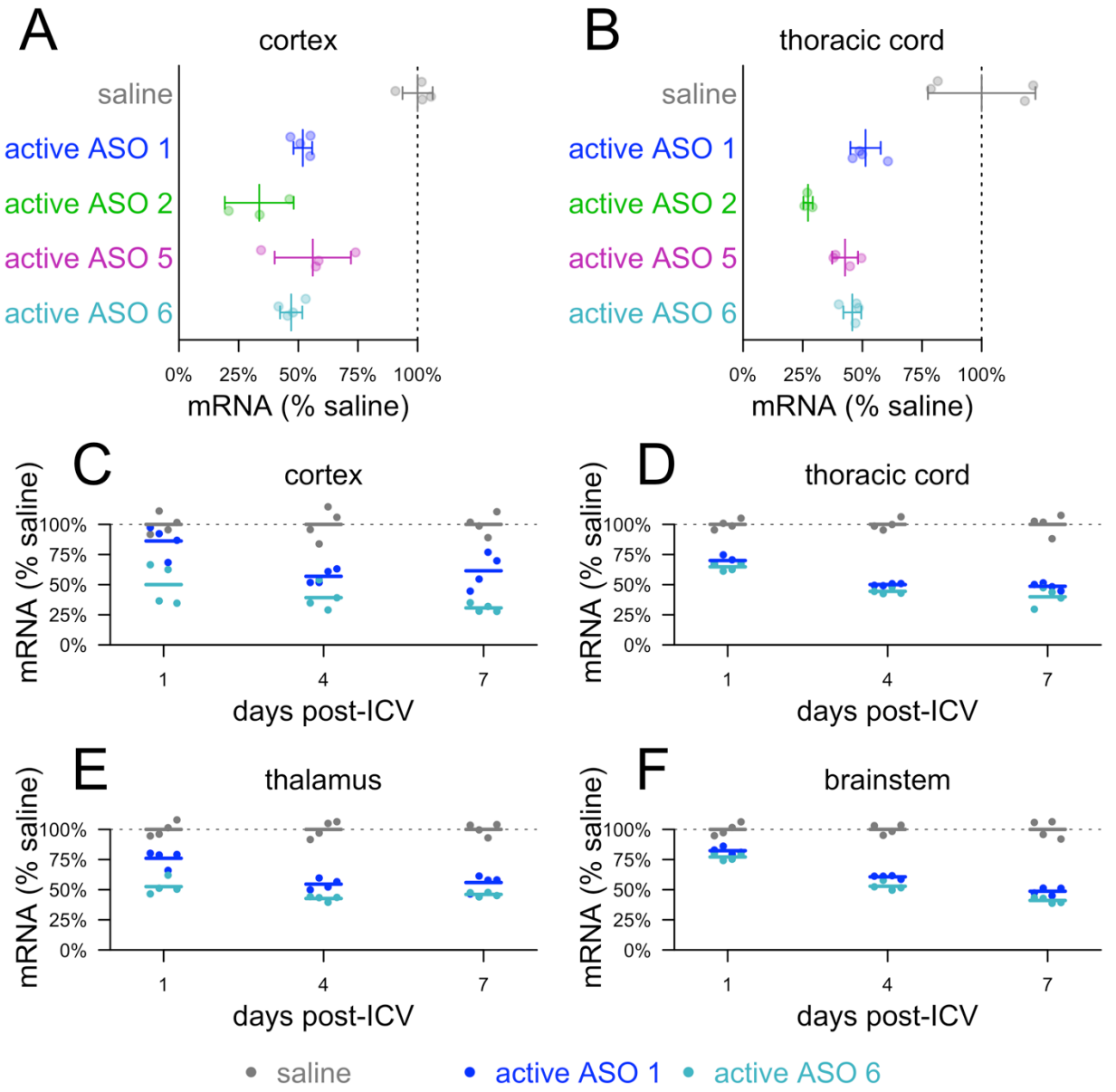

Figure S1. Potency and time-to-effect of ASOs used in this study. A-B) *Groups of N=3-4 animals received a single 700 µg dose of the indicated treatment and ipsilateral cortex (**A**) or thoracic cord (**B**) mRNA was analyzed by qPCR 8 weeks later. **C-F**) Groups of N=4 animals received the indicated ASO and ipsilateral cortex (**C**), thoracic cord (**D**), ipsilateral thalamus (**E**), or brainstem (**F**) were analyzed by qPCR 1, 4, or 7 days later.*

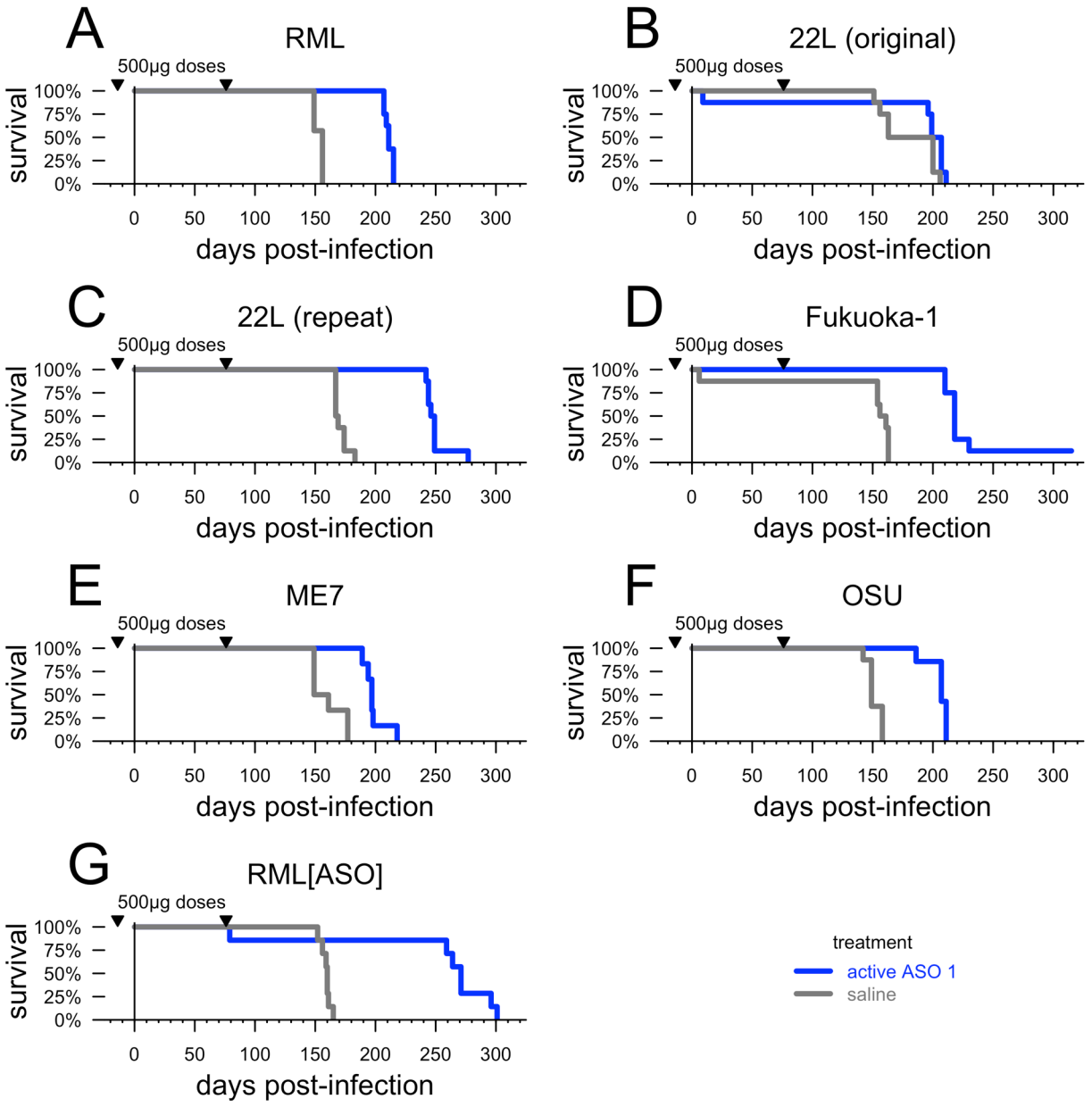

Figure S2. Survival curves for prophylactically ASO-treated animals across prion strains. *Data summarized in Table 1. In the original 22L experiment (B), we observed only a marginal increase in survival time in ASO-treated animals (+12%, P = 0.09, two-sided log-rank test). We suspected an experimental error because the distribution of survival times was bimodal among control animals: 4/4 saline-treated animals in one cage succumbed at 158±6 dpi, while 4/4 saline-treated animals in the other cage succumbed at 202±3 dpi. This latter cage had been labeled "E" while an adjacent active ASO-treated cage had been labeled "F", leading us to suspect the two cage cards had been swapped and that some of the 22L control animals had in fact received one dose of ASO. We repeated the experiment, again with blinded veterinary technicians performing all animal evaluations, and obtained the result in panel (C), which is summarized in Table 1.*

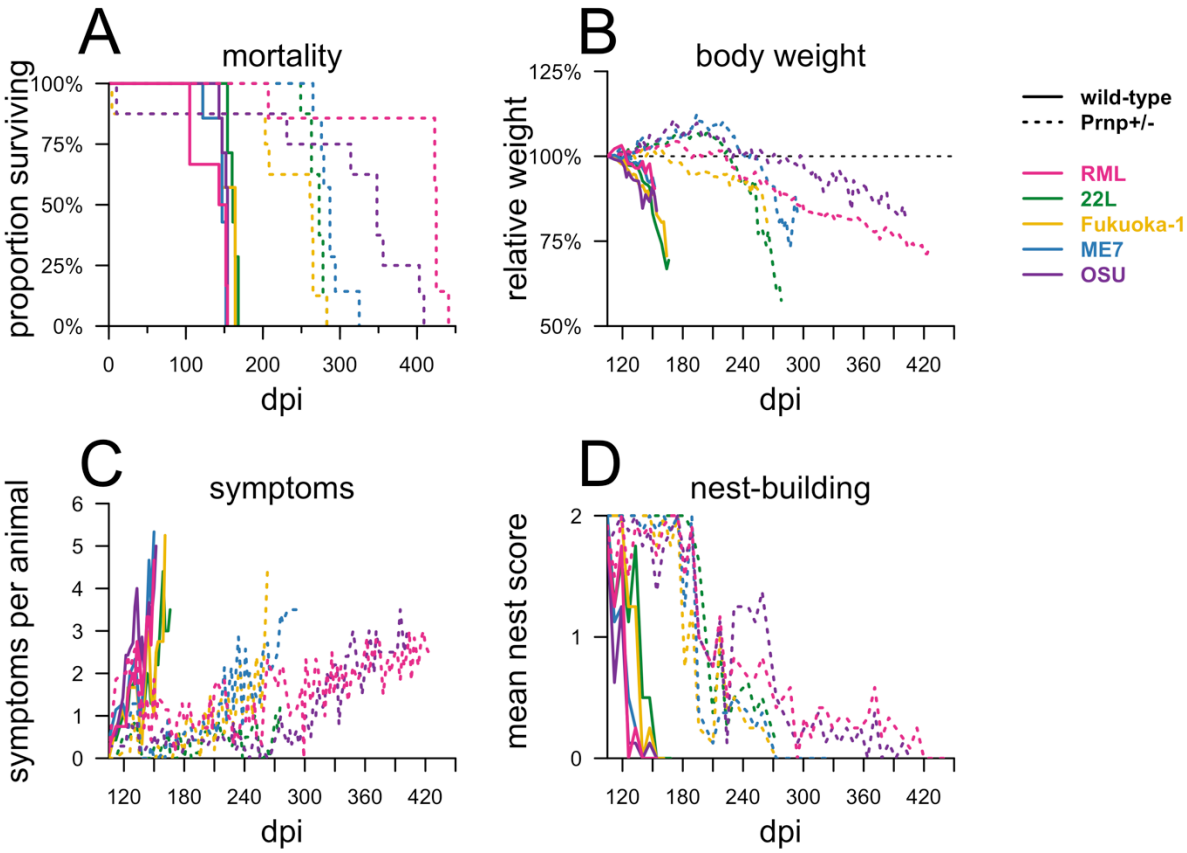

Figure S3. Endpoints in heterozygous PrP knockout mice infected with five prion strains. *Details on animals summarized in the right half of Table 1.* ***A)*** *survival,* ***B)*** *body weights relative to 105 dpi baselines (relative rather than absolute weights are used because the cohorts contain different proportions of male and female mice),* ***C)*** *mean symptom count per animal, and* ***D)*** *mean nest score.*

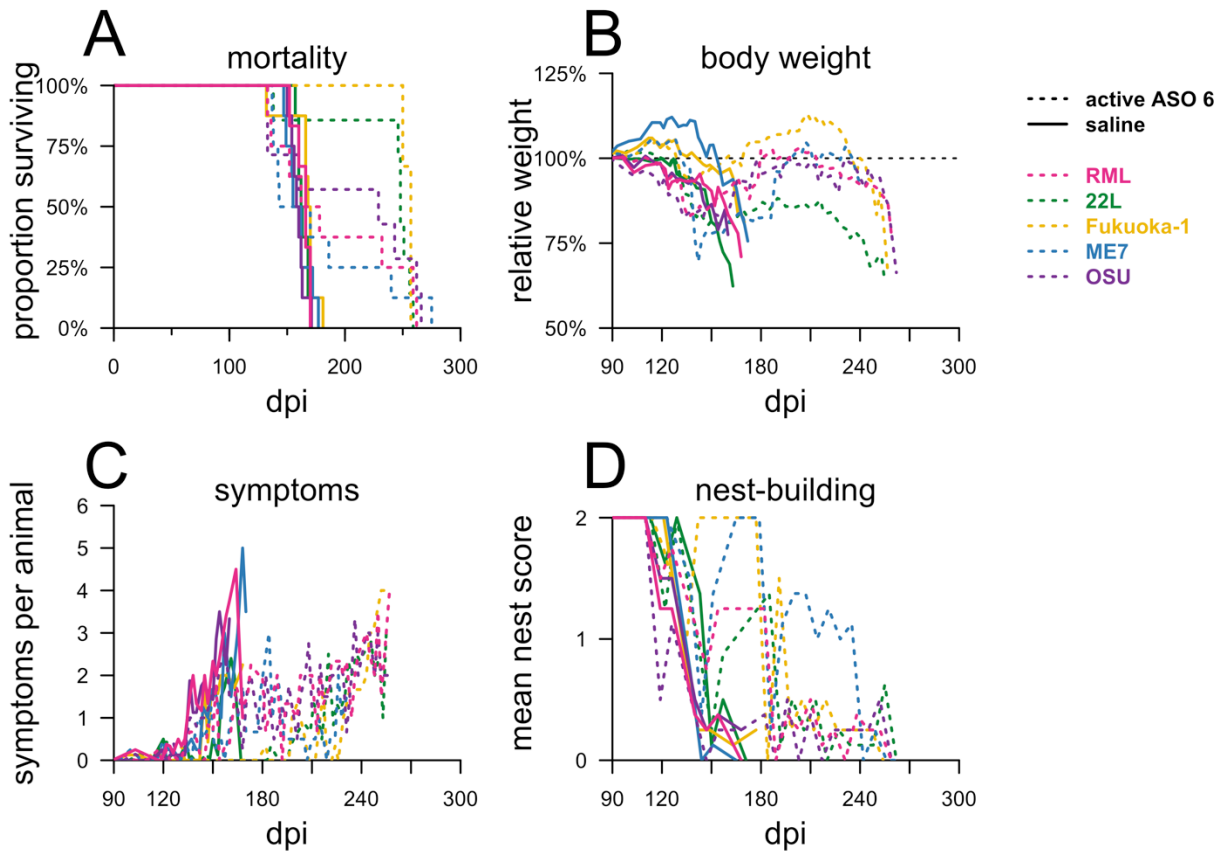

Figure S4. Endpoints in mice infected with five prion strains receiving late ASO or saline treatment. *Details on animals summarized in Table 2.* ***A)*** *survival,* ***B)*** *body weights relative to 105 dpi baselines,* ***C)*** *mean symptom count per animal, and* ***D)*** *mean nest score.*

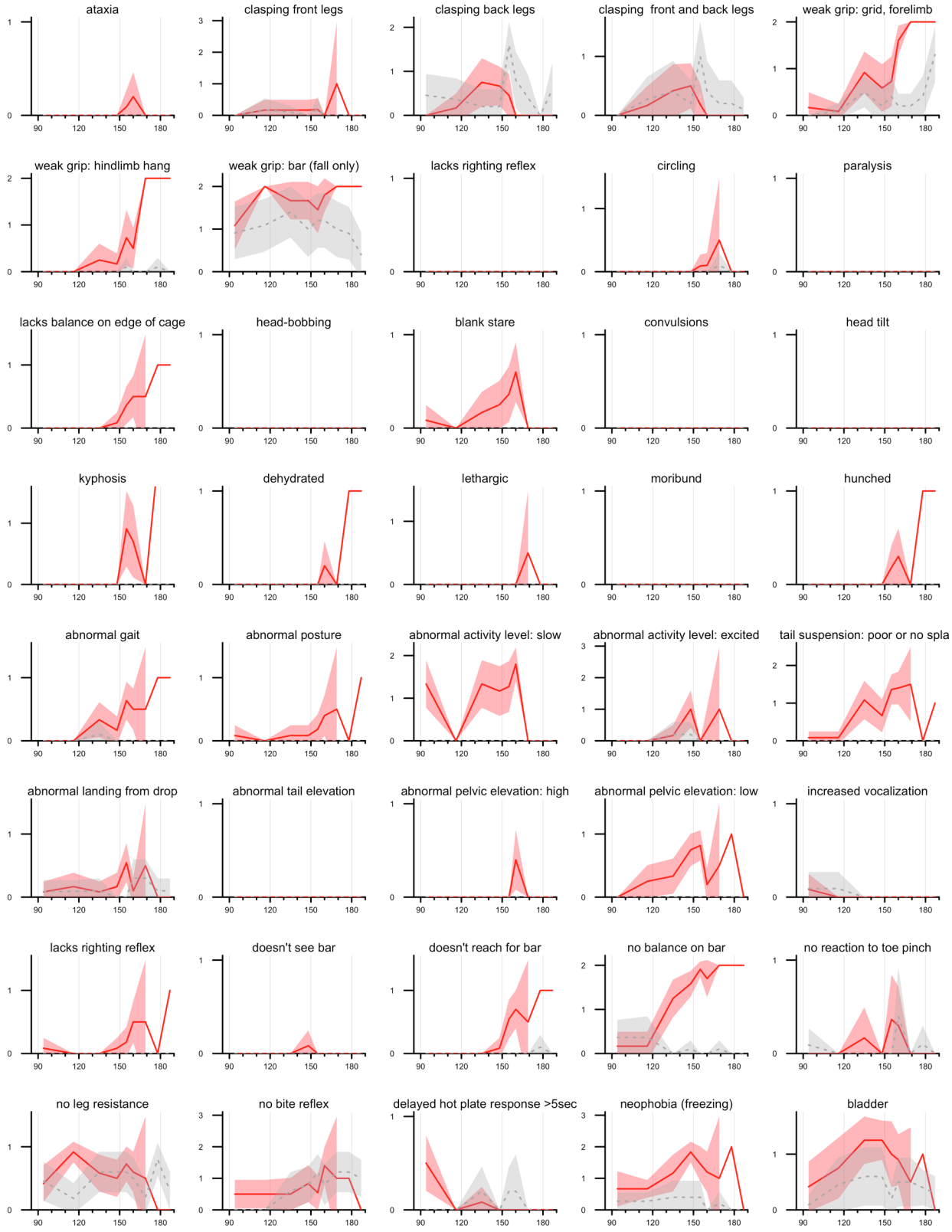

Figure S5. Behavioral observations in the natural history of RML prion infection. *Data from Figure 3C broken into all N=40 Individual behavioral observations (listed in Table S2).*

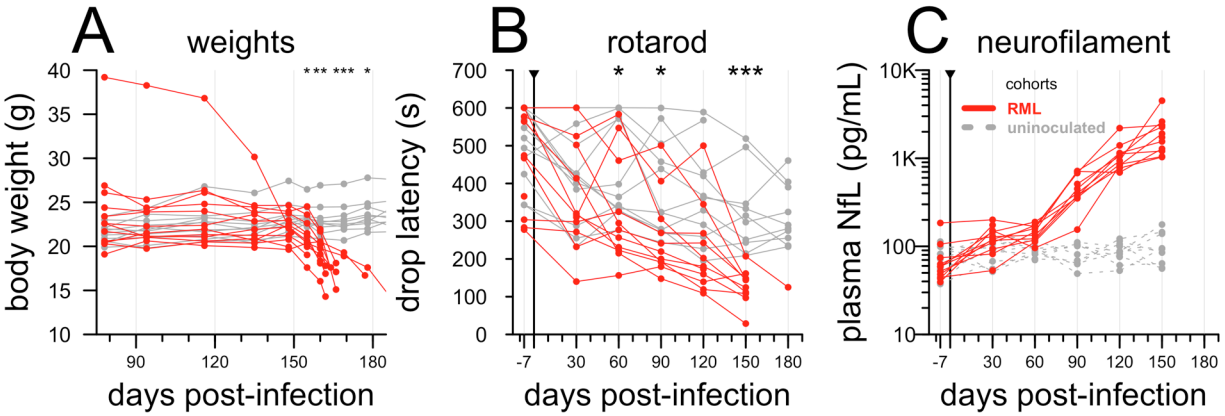

Figure S6. Raw individual natural history endpoints. *Alternative visualizations of data from Figure 3:* ***A)*** *individual body weights,* ***B)*** *individual mean rotarod latency, and* ***C)*** *individual plasma NfL concentrations (note log y axis).*

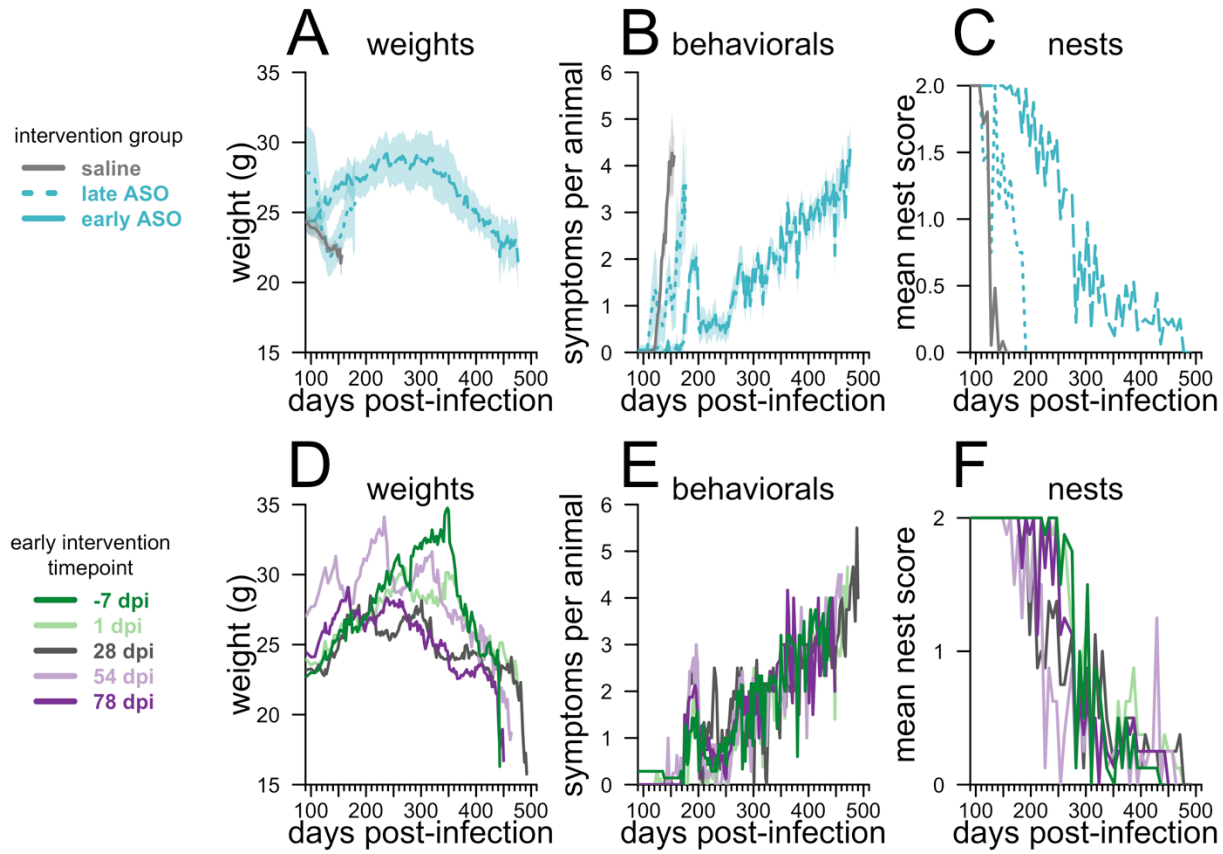

Figure S7. Endpoints in mice receiving chronic ASO or saline treatment beginning at different timepoints. *Details on animals summarized in Figure 5: weights (****A,D****), mean symptom count per animal (****B,E****), and nest score (****C,F****).* ***A-C****) animals are grouped by saline or early (-7 to 78 dpi) versus late (105 and 120 dpi) ASO treatment initiation, as in Figure 5B.* ***D-F****) early intervention (-7 to 78 dpi) animals are grouped by individual intervention timepoint.*

Table S1. Compounds used in this study. *ASOs 1, 2, 3, 4, and 6 have been previously described[28,49]. Color code for ASO chemical modifications: black = unmodified deoxyribose (2'H). orange = 2' methoxyethyl (MOE). blue = 2'-4' constrained ethyl (cET). Unmarked backbone linkages = phosphorothioate (PS); linkages marked with o = normal phosphodiester (PO). mC = 5-methylcytosine.*

ASO	sequence and chemistry	target
active ASO 1	mCToAoTTTAATGTmCAoGoTmCT	*Prnp* 3'UTR
active ASO 2	TToGomCAATTmCTATmComCoAAA	*Prnp* intron 2
control ASO 3	mComGomCTATAmCTAATomCoATAT	none
control ASO 4	mCmCoToAoTAGGAmCTATmCmCAoGoGoAA	none
active ASO 5	TToGomCoAATTmCTATmCmCAAoAoTAA	*Prnp* intron 2
active ASO 6	mCToTomCoTATTTAATGTmCAoGoTmCT	*Prnp* 3' UTR

Table S2. Measures observed in the natural history study.

category	observations	scoring
neurological	ataxia	1: difficulty getting across cage and /or falling over
neurological	clasping front legs	1: almost 2: full clasp
neurological	clasping back legs	1: almost 2: full clasp
neurological	clasping front and back legs	1: almost 2: full clasp
neurological	weak grip: grid, forelimb	1: weak or moderate 2: absent
neurological	weak grip: hindlimb hang	1: moderate (fall 1 out of 2 times) 2: weak fall 2 out of 2 tries (2x)
neurological	weak grip: bar (fall only)	1: moderate (fall 1 out of 2 times) 2: weak fall 2 out of 2 tries (2x)
neurological	lacks righting reflex (flipped on back by tail, not contact right reflex)	1: poor: all but head will roll over when tail is twisted. 2: lacking: can't right
neurological	circling	1: present
neurological	paralysis	1: paresis (limited range of motion for walking only, curled paw may be present, one limb non-weight bearing) 2: paralysis (cannot move)
neurological	lacks balance on edge of cage	1: present
neurological	head-bobbing	1: present
neurological	blank stare	1: present at initial box evaluation
neurological	convulsions	1: present
neurological	head tilt	1: present
neurological	kyphosis	1: slight to moderate 2: severe
non-neurological	dehydrated	1: present when nape pinched and/or sunken eyes
non-neurological	lethargic	1: present (immobile even after poked by finger)

non-neurological	moribund	1: present (near death)
non-neurological	hunched	1: present, not kyphosis, front and hind feet are close together when standing, not applicable to resting posture
SHIRPA	abnormal gait	1: wobble due to wide hind limb stance
SHIRPA	abnormal posture	1: present
SHIRPA	abnormal activity level: slow	1: present in home box only 2: no exploring in test box
SHIRPA	abnormal activity level: excited	1: moderate (noticed in home box or behavior box) 2: severe, may include jumping
SHIRPA	tail suspension: poor or no splay	1: poor 2: none or abnormally wide
SHIRPA	abnormal landing from drop	1: falls on tail or back from bar only (not drop from tail suspension)
SHIRPA	abnormal tail elevation	1: present
SHIRPA	abnormal pelvic elevation: high	1: present
SHIRPA	abnormal pelvic elevation: low	1: present
SHIRPA	increased vocalization	1: present
SHIRPA	lacks righting reflex	1: lacking
SHIRPA	doesn't see bar	1: present
SHIRPA	doesn't reach for bar	1: present
SHIRPA	no balance on bar	1: moderate: can balance after multiple tries or can only balance a second or two. 2: cannot balance
SHIRPA	no reaction to toe pinch	1: flinch 2: no reaction (zero: pulls paw away immediately)
SHIRPA	no leg resistance	1: doesn't react to pressure against paws (zero if any paw pushes back)
SHIRPA	no bite reflex	1: poor: notices but doesn't bite 2: no reaction (normal is immediate bite)
SHIRPA	delayed hot plate response >5sec	1: longer than 5 seconds
SHIRPA	neophobia (freezing)	1: any episode of freezing in test box (vs home box) 2: paralyzing fear
SHIRPA	bladder	0: not palpable (np) or good abdominal tone (gt), 1: small or medium 2: large or huge.

Table S3. Survival times by treatment timepoint in chronic dosing study. *Data from Figure 5 presented in tabular format. Note use of mean±sd as opposed to median in Results text. Inclusion criteria for survival are described in Methods > Statistical analysis.*

	saline		active ASO 6		
timepoint	**survival dpi (mean±sd)**	***N***	**survival dpi (mean±sd)**	***N***	Δ
-7	143±4	7	393±61	7	+174%
1	145±3	8	445±49	7	+207%
28	145±11	6	426±109	7	+194%
54	150±5	8	386±103	7	+157%
78	149±7	7	400±56	7	+169%
105	151±4	8	163±31	8	+8%
120	152±7	8	168±13	8	+11%

Table S4. Survival times by treatment timepoint in symptomatic intervention study. *Data from Figure 6 presented in tabular format. Inclusion criteria for survival are described in Methods > Statistical analysis.*

	saline		active ASO 6		
timepoint	**survival dpi (mean±sd)**	***N***	**survival dpi (mean±sd)**	***N***	Δ
120	167±9	12	211±62	12	+27%
132	162±12	11	173±50	12	+6%
143	168±7	12	198±54	11	+18%
156	164±5	6	164±4	10	0%